

1 **Title:**

2 **Identification of β 2 microglobulin, the product of**
3 **B2M gene, as a Host Factor for Vaccinia Virus**
4 **Infection by Genome-Wide CRISPR genetic**
5 **screens**

6

7 Short title: B2M in Vaccinia virus infection

8

9 Alejandro Matía (1,*), Maria M. Lorenzo (1,*), Yolimar C. Romero-Estremera
10 (1,+), Juana M. Sanchez-Puig (1), Angel Zaballos (2) and Rafael Blasco(1,**)

11

12 * These authors contributed equally to this work

13

14 **1** Departamento de Biotecnología, Instituto Nacional de Investigación y
15 Tecnología Agraria y Alimentaria – Consejo Superior de Investigaciones
16 Científicas (INIA – CSIC), Madrid, Spain

17 **2** Unidad de Genómica, Centro Nacional de Microbiología-ISCIII, Madrid, Spain,

18 + Present address: University of Puerto Rico, Medical Sciences Campus. Paseo
19 Dr. Jose Celso Barbosa, San Juan, 00921.

20

21 ** Address Correspondence to:

22 blasco@inia.csic.es; Tel.: +34-91-347-3913

23

24

25 **Abstract**

26

27 Genome-wide genetic screens are powerful tools to identify genes that act as
28 host factors of viruses. We have applied this technique to the analyze the
29 infection of HeLa cells by Vaccinia virus, in an attempt to find genes necessary
30 for infection. Infection of cell populations harboring single gene inactivations
31 resulted in no surviving cells, suggesting that no single gene knock-out was
32 able to provide complete resistance to Vaccinia virus and thus allow cells to
33 survive infection. In the absence of an absolute infection blockage, we explored
34 if some gene inactivations could provide partial protection leading to a reduced
35 probability of infection. Multiple experiments using modified screening
36 procedures involving replication restricted viruses led to the identification of
37 multiple genes whose inactivation potentially increase resistance to infection
38 and therefore cell survival. As expected, significant gene hits were related to
39 proteins known to act in virus entry, such as ITGB1 and AXL as well as genes
40 belonging to their downstream related pathways. Additionally, we consistently
41 found β_2 -microglobulin, encoded by the B2M gene, among the screening top
42 hits, a novel finding that was further explored. Inactivation of B2M resulted in
43 54% and 91% reduced VV infection efficiency in HeLa and HAP1 cell lines
44 respectively. In the absence of B2M, while virus binding to the cells was
45 unaffected, virus internalization and early gene expression were significantly
46 diminished. These results point to β_2 -microglobulin as a relevant factor in the
47 Vaccinia virus entry process.

48

49

50

51 **Author summary**

52 Orthopoxviruses, a genus belonging to the family *Poxviridae*, include human
53 pathogens like Variola virus, the causative agent of the now eradicated
54 Smallpox, and Monkeypox virus that cause human outbreaks of zoonotic origin.
55 Being the prototype Poxvirus, *Vaccinia virus* has been extensively used as the
56 ideal model to study infection. For Poxviruses, both fluid phase endocytosis and
57 direct fusion at the plasma membrane have been described as modes of entry.
58 To date, only a few cellular factors have been identified in the vaccinia virus
59 entry pathway. In this study, we report that blind genome-wide genetic screens
60 allowed us to identify several cellular factors involved in Vaccinia Virus infection,
61 of which many could be related to known factors in virus entry. In addition, we
62 found that β_2 -microglobulin constitute a novel player for Poxvirus entry not
63 related to previously described cellular pathways involved in the entry process.
64 These findings add new information to the complex picture of Poxvirus entry
65 and open the door to the discovery of new entry mechanisms used by
66 Poxviruses.

67

68

69

70

71

72 **Introduction**

73 Poxviruses are dsDNA virus whose replication cycle occur entirely in the
74 cytoplasm of the host cell (1, 2). Among the Poxviruses, Vaccinia virus (VV) –
75 which was long used as vaccine against Smallpox- is the prototype poxvirus,
76 and is the best characterized member of the family (1).

77 VV entry into cells is a complex process that has been subject to numerous
78 studies. The VV size -approximately 360 nm of diameter- has led to the
79 assumption that its entry into the cell cannot happen through caveolin or clathrin
80 vesicles (3). VV attachment to the cell is thought to occur with
81 glycosaminoglycans and laminin (4, 5). Also, several membrane proteins have
82 been proposed to serve as VV entry receptors, co-receptors or functional
83 signaling ligands (6-8), in a process that leads to VV internalization through fluid
84 phase endocytosis (9-13) followed by membrane fusion. As an alternative route,
85 direct membrane fusion at plasma membrane has also been found to be a way
86 of VV entry to the cytoplasmic space (14-17). Surprisingly, VV entry process
87 varies significantly between different cell lines, virus strains and viral forms (3,
88 16, 18-20). Taken together, these observations point to the existence of several
89 pathways leading to VV entry, which probably contribute to the broad tropism
90 range of VV.

91

92 Genome-wide genetic screens have become an important tool to identify factors
93 that are involved in biological processes. Several technologies, like RNA
94 interference or insertional inactivation have been used to carry out high
95 throughput screens. Recently, tools for the use of CRISPR/Cas gRNA libraries

96 have allowed for a more targeted way of screening genes by inactivation, down-
97 regulation or induction. Several high-throughput screenings using
98 CRISPR/Cas9 technology have been performed to target cellular factors
99 involved in infection viruses like SARS-CoV-2, West Nile virus, Influenza A
100 virus, Human cytomegalovirus and Zika virus among others, revealing many
101 host cell factors involved in viral infection (21-26). In order to unravel the
102 complexity of virus-cell interactions in Poxvirus infection, both RNAi (27-30) and
103 retroviral-mediated insertional mutagenesis DNA (31, 32) have been performed.
104 Overall, the most important hits from those studies include entry factors and
105 cellular genes somehow involved in viral morphogenesis.

106

107 We have developed a genome-wide CRISPR/Cas9-based screening using a
108 human genome wide sgRNA GeCKO library that depends on Cas9 expression
109 and delivery of a sgRNA library into cells for target gene deletion (33, 34). The
110 GeCKO library, designed to target all the genes of the human genome was
111 used to obtain a pooled population of single-gene knock-outs that was then
112 subject to Vaccinia virus infection. Through this approach, we have identified
113 B2M as a pro-viral factor related to Vaccinia virus entry. Notably, B2M encodes
114 the well characterized β_2 -microglobulin, a molecular chaperone known to form
115 complexes with multiple partners, including HLA, HFE, FcRn, MR1 (Human
116 Leukocyte Antigen, Hereditary hemochromatosis protein, Neonatal Fc Receptor
117 and Major histocompatibility complex class I-related gene protein). For those
118 proteins, interaction with B2M is needed to reach the cell membrane (35-38).
119 We show herein that inactivation of B2M gene greatly impairs VV infection and
120 viral production by affecting viral entry.

121

122 **Results**

123

124 **Genetic screen reveals a set of hits potentially involved** 125 **in VV infection.**

126

127 A loss of function, genome-wide screen was carried out by infecting a pooled
128 population of cells harboring single gene KOs. The cell population was obtained
129 by using a lentiviral library of 123,411 sgRNAs covering 19,050 genes and
130 1,864 miRNAs in the human genome (33). HeLa cells constitutively expressing
131 Cas9 were transduced with the lentiviral-sgRNA library, and passaged for 7-14
132 days in selective media. Of note, inactivation of genes essential for cell survival
133 or growth are eliminated by this procedure, and therefore the screen is directed
134 to the part of the genome that is non-essential in cell culture, which constitutes
135 about 90% of the cellular genes (39, 40).

136

137 We initially screened for gene KOs that could render the cells resistant to VV
138 infection (Fig 1). However, several experiments performed by infecting with VV
139 strain WR under various multiplicities of infection resulted in complete cell death
140 at 48-72 h.p.i. Even low m.o.i. infection resulted in no surviving cells, indicating
141 that no single gene KO was sufficient to completely block infection. This result
142 was consistent with a possible lack of complete resistance to infection by gene
143 inactivation, in agreement with previous results (32). Given that the replicative
144 strain WR was used, we reasoned that even if some degree of resistance would
145 be present in certain cells in the pool, the progeny virus in the cultures could
146 result in the death of initially surviving cells because of a second round of

147 infection. In any event, based on these results, we concluded that probably only
148 partial resistance could be achieved by single gene inactivations.

149

150 **Fig 1. Design of the pooled genetic screen for the identification of VV pro-**
151 **viral factors.** A pool of cells with single gene inactivations was obtained by
152 transducing the GeCKO sgRNA lentiviral library. After infection, surviving cells
153 are analyzed by high-throughput sequencing of the sgRNA region in the
154 integrated lentiviral construct, which is amplified by PCR. Finally, results are
155 analyzed using MaGeCK and ScreenBEAM algorithms for hit determination.

156

157 To search for pro-viral genes whose inactivation might lead to partial resistance
158 to infection, we adapted our screen by introducing three main modifications: 1)
159 we aimed at using large cell populations and controlled m.o.i. to infect only a
160 portion of the cells, 2) we performed several consecutive rounds of infection to
161 enhance the enrichment effect and 3) we used viruses with limited replication or
162 production of extracellular virus to prevent death of the surviving cells by
163 infection with progeny virus.

164

165 For the ensuing experiments, viruses with limited spread ability in the culture
166 were used. A virus deficient in genes A27L and F13L (V- Δ A27- Δ F13), which
167 has a defect in the production of extracellular virus particles limiting its
168 transmission (41, 42); and a virus deficient in the D4R gene (V- Δ D4), which is
169 blocked in DNA replication of the viral genome and therefore is unable to
170 generate infectious progeny virus (43). In the case of the latter, a
171 complementing HeLa cell line constitutively expressing VV D4 protein (HeLa-

172 D4) was engineered to allow virus expansion in a similar way to previously
173 reported (44). Using those two virus mutants and different m.o.i.s, a number of
174 experiments were completed (Table S1), in which surviving cells were
175 expanded, and analyzed. In parallel, uninfected cells were passaged for two
176 weeks and used as control.

177

178 High throughput sequencing results for the sgRNA region amplified by PCR
179 were subjected to bioinformatics analysis. Our computational analysis using
180 MaGeCK (45, 46) algorithm allowed us to identify genes that were enriched. Fig
181 2A shows the analysis of a particular experiment and Table S2 the results from
182 all experiments. In parallel, passages of non-infected cell cultures pointed to
183 gene inactivations leading to self-enrichment, with similar results to current
184 databases (i.e. DepMap Portal) (47). The degree of enrichment in infected
185 versus non-infected cells led to a refined list of possible pro-viral genes. We
186 obtained a curated hit list selecting those candidates with a False Discovery
187 Rate (FDR) < 0.05 in MaGeCK analysis, which is a narrow confidence
188 threshold. We also used ScreenBEAM algorithm (48) obtaining similar results
189 as with MaGeCK (Table S3). The results from different infection experiments
190 and from the control uninfected cultures is summarized in Fig 2B.

191

192

193 **Fig 2. Hit identification.** (A) Example of results obtained in one screen
194 experiment analyzed with MaGeCK. Hits with FDR < 0.05 are labelled with
195 gene name tags. (B) Heatmap summarizing the 27 experiments/experiment
196 variations. Genes with FDR < 0.05 in at least 1 experiment are included. The

197 results of enrichment after selection is shown in the left panel as a heatmap
198 representing the gene rank obtained with MaGeCK. For comparison, the right
199 panel shows the log₂-fold change for each gene in non-infected control
200 experiment. Dots to the right of the red dotted line indicate enrichment in non-
201 infected cultures. For instance, CMIP KOs are depleted from the pool during
202 passages in the absence of infection, whereas CSK KOs are enriched

203

204

205 **Functional protein networks.**

206 Gene hits from multiple experiments were analyzed using the ReactomePA
207 software to identify regulatory pathways (Fig. 3, Fig. 4 and Table S4). Several
208 high significance hits (FDR < 0.05 and LFC > 0) included genes previously
209 described to play a role in the initial steps of VV infection such as *ITGB1* or *AXL*
210 (6, 8), as well as genes encoding proteins involved in their downstream
211 pathways. For instance, integrin alpha subunits and actin cytoskeleton
212 remodeling proteins (*ACTG1*, *WASF2*, *ARPC2*, *ARPC3*, *ARPC4*...) are related
213 to the *ITGB1/AXL* and *AKT* activation pathway (Fig 3). Other of our strongest
214 hits is *CMIP*, a poorly studied gene that is downstream-related to *ITGB1*
215 pathway (49, 50). Although weaker hits, two annexins were also identified with
216 ScreenBEAM algorithm (*ANXA2* and *ANXA8L2*), as was a member of the S100
217 family (*S100A5*) known to interact with annexins (51, 52) (Table S4). Annexins
218 are commonly used to block phosphatidylserine due to its specific binding, and
219 have been shown to reduce VV infectivity when pretreating VV mature virion
220 with Annexin 5 (12).

221

222 **Fig 3. Screen hits related to the ITGB1/AXL activated AKT pathway.**

223 Proteins marked with a dot were hits in the screen analysis (MaGeCK: green
224 dots; ScreenBEAM: blue dots). Activation of AKT by ITGB1 signaling pathway
225 results in actin cytoskeleton reorganization, leading to VV endocytosis. CMIP
226 and AHR are new suggested players in the pathway (see main text).

227

228 **Fig 4. Pathway analysis.** Reactome Pathway Analysis was performed using
229 the top 1 % list of genes according to MaGeCK rank. Class I MHC mediated
230 antigen processing & presentation pathway was the most enriched pathway
231 with 12 genes and p-adjust value < 0.05. Genes associated to this pathway by
232 ReactomePA were B2M, UBE4A, CUL3, KLHL22, PSME1, UBE2F, RNF41,
233 PSMC3, TRIM4, PSMA8, TRIP12, ASB17.

234

235 Other hits were related to additional pathways known to be important during
236 infection, like the proteasome-ubiquitin pathway. KCTD5 emerged as one of the
237 strongest hits, although it showed some enrichment in uninfected controls.
238 Remarkably, this KCTD5 protein has been proposed to be an adaptor for cullin3
239 ubiquitin ligases and is known to modulate the activity of Rac1 protein, a
240 GTPase involved in VV internalization (53, 54).

241

242 Interestingly, B2M (the gene encoding β_2 -microglobulin) was among the best
243 hits. When analyzing the top 1% genes in the MaGeCK rank by Reactome
244 Pathway Analysis (55) the B2M-related 'Class I MHC mediated antigen
245 processing & presentation' pathway was the most prominent (Fig 4 and Table
246 S4). Enriched genes associated to this pathway were B2M, UBE4A, CUL3,

247 KLHL22, PSME1, UBE2F, RNF41, PSMC3, TRIM4, PSMA8, TRIP12, ASB17.

248 All of them except for B2M belong to proteasome/ubiquitin ligases pathway,

249 whereas B2M is more related to post antigen-processing and class I MHC

250 loading stage.

251

252 Given that B2M likely represented a novel pathway in VV entry, we reviewed

253 the screening results to check if genes related to B2M were also positive in the

254 screen. Notably, although with lower significance, *TAPBP* was detected in

255 ScreenBEAM analysis (Table S3). Other B2M related genes coding proteins like

256 Antigen peptide transporter 2 (TAP2), Protein disulfide-isomerase A6 (*PDIA6*)

257 and BiP chaperone (*HSPA5*) had good scores, even though their respective

258 FDRs (MaGeCK) or ranking criteria (ScreenBEAM) were below our initial cutoff.

259 Those results reinforce the notion that B2M and its related pathway are bona-

260 fide pro-viral factors as revealed by the survival screen. B2M protein is known to

261 bind a number of proteins that include HLA molecules, HFE or FcRn. We

262 individually tested the scores for those genes but did not find any of those

263 significantly enriched in the screening. Notably, published results on

264 experimental infections of B2M deficient mice reported unexpected levels of

265 resistance to VV (56, 57), phenotypes that now might be reasoned to be

266 influenced by B2M absence.

267

268 ***B2M* KO strongly impairs VV infection.**

269 The screen results point at B2M as a relevant novel factor in VV infection. To

270 further study its role in VV infection, we obtained HeLa and HAP1 KO cell lines

271 by CRISPR/Cas9-mediated gene-inactivation. Inactivation of B2M gene was

272 confirmed by sequencing of the mutated region in HeLa and HAP1 cells lines,
273 and loss of expression was followed by Western blot and immunofluorescence
274 analysis in HeLa clones (Fig 5A and 5B). Low multiplicity infections (m.o.i. =
275 0.05) of those clones led to a decrease in progeny virus, indicating an effect of
276 B2M absence on VV infection (Fig 5C). Those results were confirmed in two
277 independent cell clones (2.18- and 1.64-fold reduction). Those results were also
278 confirmed in the background of a second cell line, HAP1.

279

280 **Fig 5. Effect of B2M KO on VV replication.** (A) Analysis of cell lysates using
281 anti-B2M antibody. (B) Immunofluorescence images of HeLa and HeLa-B2M
282 KO cells labelled with anti-B2M antibody. (C) Virus production in HeLa and
283 HeLa-B2M KO. Infected cell monolayers (m.o.i. = 0.05) were collected 30 h.p.i.
284 and VV titers were obtained by a standard plaque infectivity assay. Error bars
285 indicate SD of three independent experiments. D and E: HAP1 and derived cell
286 lines were infected at m.o.i. = 0.05. At different time points, a fraction of
287 supernatant was collected to determine extracellular virus production (D). Error
288 bars indicate SD of three independent experiments. In the same cultures,
289 fluorescence images were obtained at different times (E). p-values: **** <
290 0.0001, *** < 0.001, ** < 0.01, * < 0.05, ns > 0.05.

291

292 Since ITGB1 has been described to be involved in VV entry (6), we were
293 interested in studying whether the function of B2M and ITGB1 are overlapping.
294 Infection of ITGB1 KO, B2M KO, and B2M/ITGB1 double KO (DKO) cell clones
295 in the HAP1 cells at low m.o.i. with a GFP-expressing VV revealed a significant
296 reduction associated with B2M inactivation, and a smaller effect associated to

297 ITGB1 inactivation, as measured by both viral production and GFP expression
298 (Fig 5D and 5E). Concurrent inactivation of B2M and ITGB1 genes did not
299 result in enhanced reduction when compared with B2M inactivation alone. We
300 additionally tested if plaque size or number were affected by inactivation of
301 B2M. For this, a GFP-expressing VV was used in a standard plaque assay in
302 the HeLa B2M KO cells. At 24 hours after infection, there was a reduction of
303 60% approximately in the number of plaques (Fig 6A). In addition, plaque size
304 was clearly diminished (Fig 6B). Overall, these results indicate that VV
305 replication was being negatively affected by B2M inactivation.

306

307 **Fig 6. Vaccinia virus plaque assay in HeLa and B2M KO cells.** MW6 well
308 plaques with HeLa and B2M KO clones 1 and 2 were infected with 200 pfu/well
309 of VV-GFP. Plaques were counted at 24 h.p.i (A). Error bars indicate SD of
310 three independent experiments. p-values: **** < 0.0001, *** < 0.001, ** < 0.01, *
311 < 0.05, ns > 0.05. (B) Images of representative plaques under the microscope
312 by GFP fluorescence.

313

314 **Effect of B2M deficiency on virus entry.**

315 We next investigated the stage in the replication cycle which was being affected
316 in B2M KO cells. We anticipated an effect on an early step in the infection cycle,
317 since viruses restricted to the early phase of the cycle (such as the D4-deficient
318 virus) result in complete cell death (not shown). We therefore hypothesized that
319 a block before that stage would be required for cell survival in the screen.
320 Consequently, we focused on the virus entry process. We used an assay based
321 on early luciferase expression (58), where an evaluation of the viral entry can

322 be assessed by the luciferase activity, which is expressed under an early
323 promoter and therefore, immediately after entry but before replication. Virus
324 entry was significantly reduced as a result of B2M inactivation, both in HeLa and
325 HAP1 cells (Fig 7A), indicating that inhibition of infection occurs at an early
326 stage in the virus cycle, before the start of DNA replication.

327

328 **Fig 7. B2M is necessary for an early stage in VV infection.** (A and B) Early
329 gene expression was taken as an indicative of virus entry. HeLa (A) and HAP1
330 (B) cells were infected with VV-Luc at m.o.i. = 0.8 and luciferase activity was
331 measured 3 h.p.i. Error bars indicate SD of three independent experiments. (C)
332 Immunofluorescence of non-permeabilized HeLa and B2M KO cells marked
333 with anti-ITGB1 showing plasma membrane expression and distribution of
334 ITGB1. (D) Absence of AXL in HAP1 cells. Cell lysates of HeLa and HAP1 cells
335 were analyzed by Western blot with anti-AXL antibody. p-values: **** < 0.0001,
336 *** < 0.001, ** < 0.01, * < 0.05, ns > 0.05. Scale bars: 20 μ m

337

338 Given the reported role of ITGB1 in VV infection, it could be reasoned that B2M
339 inactivation might result in a decrease in ITGB1 levels, which in turn would
340 inhibit VV infection. However, an indication that this might not be the case was
341 that inactivation of B2M was more inhibitory than that of ITGB1 in our
342 experimental setup (Fig 7B). Also, since B2M is required for the transport of
343 several membrane proteins from the ER to the plasma membrane, it could be
344 argued that ITGB1 transport could be affected in the absence of B2M. To
345 assess this possibility, we performed immunofluorescence with anti-ITGB1
346 antibodies in HeLa B2M KO cells (Fig 7C) Notably, ITGB1 levels in B2M KO

347 cells were similar to that in parental HeLa cells, indicating that ITGB1 was
348 transported efficiently to the plasma membrane independently of B2M.
349 Therefore, we concluded that B2M KO effect on VV infection is not mediated by
350 a decrease of ITGB1 in the cell surface.

351

352 An additional screening hit, AXL, has also been implicated in VV internalization
353 (8, 12, 32, 59). However, we do not consider likely that the B2M effect on virus
354 entry is mediated by AXL absence, since HAP1 cells do not express AXL (60).
355 This result was confirmed by Western blot, where the expression of AXL is
356 detected in HeLa but not HAP1 (Fig 7D). This result is in agreement with AXL
357 being an enhancer, albeit not an essential factor for infection (8, 61).

358

359 ***B2M* inactivation does not affect VV binding but delays**
360 **internalization.**

361 In order to test if virus attachment was affected in *B2M* KO cells we performed a
362 binding assay in HeLa *B2M* KO cells. To measure binding, purified VV particles
363 incorporating a fluorescent protein fused to a virion protein constituent (VV A4-
364 cherry) were incubated with cells and maintained at 4 °C to avoid virus
365 internalization, and virus particles bound to cells were quantitated by confocal
366 microscopy (Fig 8A and 8B). Results showed no significant differences between
367 control and *B2M* KO cells indicating no correlation between B2M presence and
368 VV attachment.

369

370 **Fig 8. VV binding is not affected by B2M absence.** (A) HeLa and B2M KO
371 cells were infected with VV A4-cherry at m.o.i = 30. After 1 h of adsorption at 4

372 °C, cells were washed with PBS and viral particles bound to the cell were
373 counted. To standardize measurements data is given in relation to cell surface
374 area. (B) Example showing the labeling with WGA-488 to visualize the cell
375 surface. p-values: **** < 0.0001, *** < 0.001, ** < 0.01, * < 0.05, ns > 0.05.
376 Scale bars: 10 µm.

377

378 We next analyzed the effect of B2M absence on the efficiency of VV
379 internalization. For this, after the initial virus adsorption period, cells were
380 incubated at 37 °C to allow virus internalization and therefore, internalized virus
381 particles were quantitated at different times (Fig 9A). We used VV A4-cherry (for
382 total virus) and an antibody targeting the VV Intracellular Mature Virion surface
383 protein A27 to detect those viral particles that were not internalized (Fig 9B).
384 Virus internalization occurred progressively over time in HeLa cells, similarly to
385 previous reports (9). Comparison with HeLa cells deficient in B2M showed a
386 consistent decrease in the internalization rate in *B2M* KO cells, an effect that
387 was more pronounced at the intermediate tested times (Fig 9A). These results
388 suggest that a delay in virus internalization exists as a result of B2M
389 inactivation, although some virus particles are eventually able to reach the cell
390 interior.

391

392 **Fig 9. B2M gene inactivation affects VV internalization.** (A and B) HeLa and
393 B2M KO cells were infected with VV A4-cherry at m.o.i. = 4 during 1 h at 4 °C to
394 avoid internalization. Cells were incubated for different times at 37 °C and non-
395 permeabilized cells were stained with antibody to VV-A27 (green) to visualize
396 cell surface virus particles. White arrow-heads mark internalized virions (only

397 red in merged image) and yellow-empty arrow-heads indicate non-internalized
398 virions (green or yellow). Cell nucleus was labeled in blue by Hoechst staining.
399 Internalized virions were quantified for each time point showing significant
400 differences between HeLa and B2M KO cell lines. p-values: **** < 0.0001, *** <
401 0.001, ** < 0.01, * < 0.05, ns > 0.05. Scale bars: 5 μ m.

402

403 **VV colocalization with B2M.**

404 As the specific role of B2M in early VV infection is related with the early steps of
405 infection, we tested the degree of colocalization of B2M and VV at cell
406 membrane. Since viral entry is a sequential process in which different protein-
407 protein interactions may occur over time (62, 63), different time points were
408 included in the experiment. After adsorption of fluorescent VV A4-cherry
409 particles at 4 °C, cells were stained with antibodies specific for B2M and ITGB1.
410 Confocal images of non-permeabilized cells revealed a partial colocalization of
411 B2M and attached virus particles (Fig 10A). We found approximately 50 % of
412 VV particles colocalizing with B2M at 0, 15, 30, 45 and 60 min post infection (S2
413 Fig). To determine if these colocalization results were consistent, we estimated
414 VV/ITGB1 colocalization, that has been described to occur, at least in HeLa
415 cells at 0 min (6). Our results showed that 38 % of adsorbed VV particles
416 colocalized with structures containing ITGB1. Also measured that 24% of B2M-
417 positive structures were also labeled with ITGB1, and that 20% of ITGB1-
418 positive structures were also labeled with B2M. Those results indicate only
419 partial colocalization of the two proteins with each other, and with the infecting
420 VV particle, and show a substantially differential pattern for B2M and ITGB1
421 (Fig 10B).

422

423 **Fig 10. VV, B2M and ITGB1 partial colocalization.** (A) HeLa cells were
424 infected with VV A4-cherry (red) for 1 h at 4 °C and unbound virus was removed
425 by washing (m.o.i. = 5). Cells were stained with anti-B2M antibody (green) to
426 analyze colocalization. Colocalization of VV with B2M is indicated with white
427 arrow-heads. (B) Non permeabilized HeLa cells were stained with anti-B2M
428 (green) and anti-ITGB1 (red) to analyze colocalization. Scale bars: 5 µm.

429

430 Finally, we wished to determine if B2M was able to block virus infection by
431 interacting directly with the virus particle. For that, purified VV particles were
432 incubated with soluble B2M and then used for infection. In those experiments,
433 no significant differences were found (S3 Fig). On the other hand, a blocking
434 assay was also performed pretreating the cells with different concentrations of
435 anti-B2M antibody, followed by VV infection but we did not observe any
436 significant blocking activity (S4 Fig).

437

438

439 Discussion

440 CRISPR/Cas9 genetic screen.

441 The interactions between VV and the host cells have been a subject of
442 considerable research. In this work, we have used CRISPR/Cas9 technology to
443 perform a pooled, genome-scale loss-of-function screen with the aim of
444 identifying cellular genes necessary for VV infection. From the design of our
445 screening, it should be noted that we are only testing the non-essential gene
446 set, since after subjecting pooled KO cell population to six passages, the cells in
447 which essential functions are inactivated are depleted from the pool. Likewise,
448 an enrichment is observed for some KOs in genes that perform functions
449 related to the control of cell proliferation and apoptosis. This observation is
450 common in screens of cellular genes (47).

451

452 The experimental approach to this problem was complicated by the
453 considerable versatility and adaptability of Vaccinia infection. In fact, in our
454 initial experiments, all cells showed cytopathic effect and suffered cell death
455 over time, regardless of the multiplicity of infection used in the experiment.
456 Failure to obtain even a single surviving cell suggests that a single KO mutation
457 is not enough to confer complete resistance in the cells. This could be due to a
458 number of different reasons. A first explanation might be that the virus is able to
459 enter the cell using different, non-overlapping molecular pathways. Second,
460 even if there is partial resistance, it may be difficult to isolate a few resistant
461 cells within a large cell population of virus-producing cells. Indeed, since the
462 bulk of the cells would remain susceptible they would generate high loads of
463 progeny virus that may overcharge and kill the partially resistant cells. In this

464 respect, it has been shown that even inactivated virus can induce cell death
465 (64). In similar approaches, high multiplicities of infection resulted in the death
466 of the whole cell population, a difficulty already reported by Luteijn et al. (32).

467

468 In view of these considerations, we modified the screening protocols to exert a
469 gradual enrichment of partially resistant cells. Those modifications included
470 infection with viruses that have decreased spread or limited replication, and
471 adjusting the multiplicity of infection to modulate the selective pressure. The
472 screening design was directed at maintaining a controlled selective pressure in
473 the form of virus-induced cell death in the cultures during extended periods.
474 Importantly, this may favor the enrichment of cells harboring gene-KOs leading
475 to enhanced cell growth, as we have seen over extensive passage of uninfected
476 samples. Therefore, enrichment in our experiments may stem from increased
477 resistance to infection or from faster cell growth. This was taken into account
478 when analyzing the possible hits in the screening by comparing sgRNA
479 changes in infected and control uninfected cultures (Fig 2B).

480

481 We have observed that viruses blocked in DNA replication, such as the V- Δ D4
482 virus mutant, efficiently promote cell death even though replication cycle is not
483 completed. This indicates that cell survival is not possible after the early stage
484 of virus infection is reached. Because our screening was based on cell survival,
485 it not surprise that it was preferentially directed to the cell entry process.
486 Vaccinia virus and Poxviruses in general are known to have a complex entry
487 process into host cells, where they first bind in an unspecific manner to
488 extracellular matrix components such as glycosaminoglycans (GAGs) and

489 laminin, followed by a more specific attachment step (4, 6, 63). During this
490 process, signal activation pathways are triggered in the cell, leading to the
491 internalization of the virus through fluid phase uptake and -to a lesser extent-
492 direct fusion at plasma membrane (7, 12, 58). With our screen approach, we
493 identified several potential gene candidates that may play a role in early stages
494 of infection. Statistically significant hits like *ITGB1* and *AXL*, as well as some of
495 their downstream pathway proteins such as Akt-pathway-related proteins, the
496 small GTPases –RhoA, Rac1, Cdc42-, or actin cytoskeleton remodeling
497 proteins (6, 8, 65-67) were obtained. Additional gene hits were also related to
498 these pathways. For instance, c-Maf activating protein (CMIP) was one of the
499 strongest hits and is thought to participate in several cellular processes,
500 including integrin expression through c-Maf activation, actin cytoskeleton
501 remodeling and the Akt route (49, 50, 68). Another hit was AhR (*AHR*), which is
502 known to be bound to c-Maf (69, 70). We suggest that CMIP may have
503 emerged as a hit in our screen due to the concurrence of the different actions
504 where this protein is involved (Akt pathway, cytoskeleton, integrin expression...)
505 (50, 71, 72). Because CMIP is a poorly studied gene, it will be of interest to
506 study its potential function in VV infection. Overall, this study contributes to
507 expand the big picture of the likely cell - VV interactions during the first steps of
508 infection.

509

510 **β_2 -microglobulin gene (B2M).**

511 Unexpectedly, B2M gene appeared as one of the strongest hits in the screen,
512 implying B2M protein is an important player in VV infection. B2M is a molecular
513 chaperone that is expressed in most mammalian cells and binds several protein

514 ligands such as MHC-I, HFE or FcRn before their transport to the cell surface.
515 We used different approaches to determine the role of B2M in VV infection.
516 First, we found that B2M deficiency leads to a decrease in viral plaques, and a
517 lower viral progeny titer. Second, B2M role is relevant during early infection
518 stages, since early gene expression was clearly diminished (Fig 7). More
519 precisely, we demonstrated that B2M absence does not affect VV binding but it
520 does decrease internalization (Fig 8 and Fig 9). Although internalization
521 differences were around 25 % between *B2M* KO and normal cells, these
522 differences were much greater in early expression luciferase assays (around 70
523 %). Several explanations may account for the difference: for instance, the
524 existence of an unproductive internalization pathway in *B2M* KO cells, not
525 leading to early transcription. Also, the internalization delay and defect in *B2M*
526 KO cells may be indicative of the inefficacy of VV virions finding their signaling
527 ligands at cell surface, therefore abrogating them to the unproductive pathway
528 above mentioned.

529

530 ITGB1, which has also been shown to be involved in VV entry, was also a
531 significant hit in the screen,. However, several results point to B2M as acting
532 independently of ITGB1. First, the effect of the inactivation of B2M in VV
533 infection in HAP1 cells was stronger than that observed ITGB1 KO.
534 Furthermore, the depletion of B2M in the HAP1-ITGB1-KO line also resulted in
535 a clear reduction of VV infectivity. This result shows that in the absence of
536 ITGB1 and AXL (the latter not being expressed in HAP1 cells), B2M is still
537 necessary for VV infection. Those results can be explained as B2M acting as a
538 key player in alternative virus entry pathway.

539

540 Pathway Analysis of the data from screening experiments showed that Class I
541 MHC mediated antigen processing & presentation pathway was the most
542 enriched one, including many proteins related to the proteasome and ubiquitin
543 system. In this respect, a screen using Monkeypox virus also pointed to several
544 enriched ubiquitin genes and other B2M-related genes, such as TAPBP and
545 CALR (31, 32). The ubiquitin system has been extensively studied for its
546 importance during infection, and its relationship to B2M is hence intriguing in
547 view of our results.

548 At this point, there is no clear mechanism to account for B2M role during
549 infection. B2M requirement for VV infection might be the result of a direct
550 involvement of this protein in the entry process. However, given that B2M forms
551 protein complexes with a number of membrane proteins, one interesting
552 possibility is that one of those complexes might act as a VV receptor or
553 internalization factor. Nonetheless, we have analyzed our screening results
554 searching for these B2M related genes, and we found no clear results. Gene
555 redundancies, in particular regarding HLA genes, may obscure the screening
556 results, that have the limitations imposed by the fact that only single gene
557 inactivations are tested. Current experiments are directed at exploring if any of
558 those B2M heterocomplexes is indeed involved in virus entry.

559

560 The known function of B2M does not offer an evident link with a mechanism of
561 virus entry. However, its function in the initial steps of VV infection is not a
562 singular case. Intriguingly, some similarities exist with Coxsackievirus A9
563 (CAV9) -an enterovirus B- whose internalization is also mediated by B2M (73-

564 75) and which also makes use of at least two subunits of integrin; beta 6 and
565 beta 3. Furthermore, CAV9 entry is mediated by dynamin, as is also the case
566 with VV (76). Recently, it has been found that the effect of B2M for Enterovirus
567 B entry can be explained by the need of B2M in mediating the transport to the
568 membrane of its receptor, the Human Neonatal Fc Receptor (FcRn) (77, 78).
569 Expanding the similarities to the case of CAV9, we obtained ASAP1 as a hit
570 (Table S3), a GTPase activating protein involved in Arf1, Arf5 and Arf6
571 activation and cytoskeleton remodeling (79), the latter of which being known to
572 mediate endocytosis for some viruses, like CAV9 (74). As authors suggested,
573 virions might undergo an unproductive entry pathway in B2M absence (74), a
574 hypothesis that is consistent with our results. Due to the several similarities in
575 cellular requirements of CAV9 and VV entry, it is likely that one of the entry
576 mechanisms for VV is shared by CAV9. In any event, more research is needed
577 to further clarify the details of the process.

578

579 One last interesting aspect of B2M involvement in virus entry is the relevance of
580 B2M product (β -2 Microglobulin) in the immune response. The involvement of
581 B2M as a pro-viral factor might have multiple consequences regarding the
582 pathogenesis and immune response in animal infection. Interestingly, two
583 reports in the literature found that B2M-deficient mice were remarkably
584 resistant to VV infection, despite the lack of cell-mediated immunity in those
585 animals as a consequence of MHC-I deficiency (56, 57). This result suggests
586 the B2M deficiency has also a VV blocking effect, even though those mice have
587 a T cell immunodeficiency.

588

589 Overall, this report adds a new player to our picture of the complex interplay
590 between cell and virus in the VV entry process. Delineation of the protein
591 interactions and pathway activations taking place in this process will
592 undoubtedly involve multiple players yet to be discovered.

593

594

595

596

597 **Materials and Methods**

598

599 **Cells.**

600 HeLa (ATCC CCL-2) cells were grown in Eagle's Minimal Essential Medium
601 (EMEM) containing 7 % fetal bovine serum (FBS). BSC-1 cells (ATCC CCL-26)
602 were grown in Eagle's Minimal Essential Medium (EMEM) with 5 % fetal bovine
603 serum (FBS). HAP1 and its derived lines (*B2M* KO, *ITGB1* KO and double
604 *B2M/ITGB1* KO (DKO)) were purchased from Horizon Discovery and were
605 grown in Iscove's Modified Dulbecco's Medium (IMDM) containing 7 % fetal
606 bovine serum (FBS). HEK-293T cells were grown in Dulbecco's Minimal
607 Essential Medium (DMEM) with 7 % fetal bovine serum (FBS). All media were
608 supplemented with 0.1 mg/mL penicillin, 0.1 mg/mL streptomycin, 2 mM L-
609 glutamine (BioWhittaker). Cells were grown in a 5 % CO₂ incubator at 37 °C.

610

611 **Viruses.**

612 Vaccinia virus (VV) Western Reserve (WR) strain was obtained from the
613 American Type Culture Collection (ATCC VR-119) and routinely propagated in
614 BSC-1 cells. Previously described viruses V-GFP (recombinant WR expressing
615 GFP) (80), and V- Δ A27 Δ F13 (recombinant having the A27L and F13L genes
616 deleted) are already described (41).

617

618 Virus infections were performed in media containing 2 % FBS. Viral titers in cell
619 lysates obtained after disrupting the cells by three rounds of freeze/thawing
620 were determined by the standard VV plaque assay in BSC-1 cells (81).

621

622 **Isolation D4R expressing cells.**

623 Complementing cell lines 293-D4rR and HeLa-D4rR were obtained by inserting
624 the VV D4R gene in the genome of the parental cells using the Flp-in T-REx™
625 system from Invitrogen. The integrative plasmid pCDNA-FRT-TO-D4R was
626 transfected in the cell line HeLa Flp-In™ T-REx™ (R71407) or 293-FITR- Flp-
627 In™ T-REx™ (R78007) and subsequently cell clones were selected for
628 hygromycin resistance. A bicistronic construct was inserted, placing the VV D4R
629 gene downstream of a tetracyclin-inducible promoter and the TagRFP gene
630 downstream of an IRES sequence. Clones generated from 293 and HeLa were
631 chosen by monitoring the appearance of red fluorescence after tetracycline
632 induction. The efficacy of cell line complementation was tested by plaque
633 phenotyping with the V-ΔD4L virus.

634

635 **Generation of recombinant and mutant vaccinia** 636 **viruses.**

637 Recombinant virus V-A4-cherry was generated as previously described (76).
638 Briefly, BSC-1 cells (6-well plate format, 10⁶ cells/well), were infected at a
639 multiplicity of infection (MOI) of 0.05 PFU/cell with virus WR. After 1 h viral
640 adsorption, virus inoculum was removed and cells were then transfected with
641 2 μg of plasmid pm-cherry-A4L (kindly provided by Wen Chang) using

642 FuGeneHD (Promega) according to the manufacturer's recommendations. After
643 2 to 3 days, cells were harvested, and recombinant virus was isolated by three
644 consecutive rounds of plaque purification. Viral stocks were generated in BSC-1
645 cells and viral titers were determined by standard plaque assay (PFU/mL).

646

647 V- Δ D4L virus was isolated following the protocol already described (43, 44) by
648 infection/transfection of BSC-1 cells with WR virus and plasmid p Δ D4R-dsRed.
649 p Δ D4R-dsRed contains the dsRed gene downstream of a synthetic early/late
650 promoter between two DNA segments acting as recombination flanks for the
651 D4L locus. At 72h the culture was collected and several successive rounds of
652 plaque purifications in BSC-1 cells were performed by selecting large red
653 plaques (representing single recombinants). The resulting virus was amplified in
654 the complementing cell line expressing the D4R gene (HeLa-D4R). The
655 amplified stock was plaque purified in the HeLa-D4R line. The size phenotype
656 for each clone was checked by plaquing in parallel in the BSC-1 line and the
657 HeLa-D4L line. Virus clones that produced large plaques in the HeLa-D4 cell
658 line and single infected cells in BSC-1 were selected.

659

660 V-e.luc VV recombinant expressing firefly luciferase under the control of an
661 early promoter was constructed by inserting an early-Luc cassette in plasmid
662 pA-E-Luc into the A27L locus using a plaque selection procedure (41).

663

664 **Lentiviruses.**

665 Lentivirus stock production was performed by cotransfection of HEK293T cells
666 with the lentiviral plasmid with the packaging plasmid psPAX2 and

667 pseudotyping plasmid pCMV-VSV-G. Plasmid psPAX2 was a gift from Didier
668 Trono (Addgene plasmid # 12260 ; <http://n2t.net/addgene:12260> ;
669 RRID:Addgene_12260). pCMV-VSV-G was a gift from Bob Weinberg (Addgene
670 plasmid # 8454 ; <http://n2t.net/addgene:8454> ; RRID:Addgene_8454). For
671 sgRNA expression, plasmids lentiGuide-Puro (Addgene plasmid # 52963 ;
672 <http://n2t.net/addgene:52963> ; RRID:Addgene_52963) or lentiCRISPR v2,
673 (Addgene plasmid # 52961 ; <http://n2t.net/addgene:52961> ;
674 RRID:Addgene_52961) provided from Feng Zhang, were used. For stock titer
675 determination, HeLa cells on MW6 plates were infected with successive
676 dilutions of the lentiviral particle stock and incubated with the corresponding
677 selective medium (blasticidin 5 µg /mL or puromycin 1 µg/mL). After cell clones
678 were visible at the microscope, titer was calculated from the number of resistant
679 clones.

680

681 **Isolation of Cas9 expressing HeLa cells.**

682 LentiCas9-Blast plasmid was a gift from Feng Zhang and was obtained from
683 Addgene (Addgene plasmid # 52962; <http://n2t.net/addgene:52962>; RRID:
684 Addgene_52962). HeLa cells grown on MW6 wells were transduced with
685 different dilutions of a lentiviral stock obtained from LentiCas9-Blast. After
686 applying selection with blasticidin (5 µg/mL) for 10 days, cell clones were visible
687 at certain dilutions from which lentiviral titers were estimated. Cells transduced
688 with an m.o.i. of 3-5 were cloned by limit dilution in MW96 wells and individual
689 clones were harvested and expanded for further analysis. Cas9 expression was
690 verified by immunofluorescence and western blotting using anti-flag antibody. A

691 cell clone with the highest Cas9 expression was termed HeLa-Cas-ML,
692 expanded and used for subsequent experiments.

693

694 **CRISPR Knock-Out (GeCKO) v2.0 libraries: lentivirus**
695 **stock and derived cell lines.**

696 The Human GeCKO v2.0 library, a gift from Feng Zhang, in the two lentiviral
697 vector version (Addgene 1000000049), was used (33, 34). The lentiviral library
698 LentiGuide-puro consists of specific sgRNA sequences for gene knock-out
699 covering the gene set of the human genome. The library is supplied as two half-
700 libraries (A and B). When combined, the libraries contain 6 sgRNAs per gene
701 (3 sgRNAs in each library).

702 HeLa-Cas-ML cells were transduced with lentiviral libraries A and B separately
703 and selected with puromycin to obtain a cell mixture called HeLa-Mix. For each
704 library, cells in 4 subconfluent T150 flasks were transduced with approximately
705 2×10^7 lentiviral particles. At 24 h, medium was replaced by fresh medium
706 containing 1 $\mu\text{g}/\text{mL}$ puromycin. After three days the cells were harvested,
707 pooled, and subcultured to 8 T225 flasks. Subsequently, cells were transferred
708 to 24 T225 flasks maintaining the selective medium at all times for 10 days and
709 constituting the pass 0.

710

711 **Genetic Screen.**

712 GeCKO KO cell pools in 2 T225 flasks (about 10^8 cells) were infected in each
713 condition. Cells were maintained in EMEM-7% FBS except during virus
714 adsorption, which was carried out in EMEM containing 2% FBS. Uninfected

715 control cells were maintained in culture for 8 subcultures before analysis.
716 Detached cells from the Infected cultures were removed regularly. Infection was
717 monitored by detecting infected cells by fluorescence (red fluorescence for V-
718 Δ D4L and blue fluorescence for V- Δ A27 Δ F13). To exert selective pressure in
719 the cultures in the form of VV infection, cells were occasionally re-infected with
720 fresh inoculum. If cultures reached confluence, they were subcultured into new
721 T225 flasks. To avoid population bottlenecks in the sgRNA population, cell
722 dilutions at each passage were never greater than 4-fold. The last passage was
723 allowed to reach confluence and the cells were harvested and prepared for
724 sgRNA quantitation in the surviving population. The conditions under which the
725 infection experiments were performed are summarized in S1 Table.

726 After the selective process, cellular DNA was extracted and the lentiviral region
727 containing the sgRNA sequence was PCR amplified and sequenced. For DNA
728 purification cell samples were suspended in 500 μ L of lysis buffer (10 mM Tris
729 (pH 8.0), 10 mM EDTA, 10 % SDS and 100 μ g/mL proteinase K) and incubated
730 3 h at 55 °C or o/n at 50 °C. Samples were then extracted with an equal volume
731 of phenol twice, then 3-5 times with a volume of phenol: chloroform: isoamyl
732 alcohol (25: 24: 1) and finally once with a volume of chloroform: isoamyl alcohol
733 (24: 1). DNA was then precipitated by adding one-tenth volume of 3 M sodium
734 acetate and two volumes of ethanol and, cooled to -20 °C for 1 h followed by 30
735 min centrifugation at 4 °C and 13000 rpm. The pellet was resuspended in 300
736 μ L TE with RNAase mix and frozen at -20 °C for storage.

737 Amplicon for sequencing was derived from cellular DNA by three successive
738 nested PCRs. PCR reactions were performed with Biotools thermostable
739 DNAPol enzyme. The first PCR was performed on all the purified DNA as

740 template, by setting up multiple reactions containing each 5 µg of DNA in 100
741 µL of reaction volume, with 5'P1, 3'P1 oligonucleotides and 15 amplification
742 cycles. After the first PCR, all reactions were pooled and a second PCR was
743 performed in four-fold less reactions with a 1:20 dilution of the first as template
744 in 100 µl of reaction with oligonucleotides 5'P2, 3'P2, and 20 amplification
745 cycles. The third PCR was performed similarly (1:20 template, 1:4 number of
746 reactions, 20 cycles) to incorporate the sequences and the barcodes
747 necessary for Illumina sequencing. Each sample carries a different combination
748 of R and F oligonucleotides in order to multiplex the Illumina sequencing run.
749 Sample libraries were equimolarly mixed and the resulting pools quantified by
750 dsDNA fluorescence (Quantifluor, Promega) and qPCR (KAPA Library
751 Quantification kit, Roche). Single-end sequencing (76 bases) was performed in
752 a NextSeq 500 (Illumina) sequencer or in a Hiseq (Illumina).

753

754 **Statistical analysis and screen data analysis.**

755 Control and infected samples read counts were analyzed with MaGeCK test
756 function (45) and ScreenBEAM algorithm (48). MaGeCK log₂-fold change (LFC)
757 scores of each gene were used for data visualization using R coding language.
758 A cutoff of FDR < 0.05 was applied for the heatmap representation to select the
759 best hits of each screen experiment. For ScreenBEAM analysis, the 20 best hits
760 were selected from each experiment following z-score criteria. Genes with less
761 than 3 successful sgRNAs as well as gene knockouts enriched in control were
762 filtered out. ReactomePA (R package) was performed using the top 1 % gene
763 list from MaGeCK output. Statistical analysis were performed using Student's *t*

764 test and one-way ANOVA (when more than two group comparisons) using
765 *Bonferroni* correction method (GraphPad Prism 8 and RStudio 1.2.5033).

766

767 **Isolation of KO cell clones.**

768 HeLa B2M KO lines: To obtain a B2M KO cell line, pLentiCRISPRv2 was
769 digested with BsmBI, and a pair of annealed oligonucleotides were cloned into
770 the single guide RNA cloning site. Two different sgRNAs for human B2M gene
771 were selected. Oligonucleotides for clone 1 were: B2M_sg1f
772 CACCGACTCACGCTGGATAGCCTCC and B2M_sg1r
773 AAACGGAGGCTATCCAGCGTGAGTC. Oligonucleotides for clone 2 were:
774 B2M_sg2f CACC. GCAGTAAGTCAACTTCAATGT and B2M_sg2r
775 AAACACATTGAAGTTGACTTACTG. Lentiviral plasmids containing B2M
776 sgRNA were obtained by cloning the hybridized oligonucleotide pairs
777 B2M_sg1f/B2M_sg1r and B2M_sg2f/B2M_sg2r to obtain plasmids
778 pLentiCRISPRv2-B2M1 and LentiCRISPRv2-B2M2 respectively. HeLa cells
779 were transduced with lentiviral preparations of LentiCRISPRv2-B2M1 or
780 LentiCRISPRv2-B2M2 and puromycin resistant clones were selected. After
781 western blotting analysis, clones that did not express B2M were selected,
782 expanded and verified by sequencing the genomic target region.

783

784 **VV entry and Blocking assays.**

785 For VV entry assays, luciferase activity driven from a VV early promoter at 3
786 h.p.i. was measured. Cells were plated in MW96 wells and incubated with VV
787 e.luc (m.o.i. = 0.8) for 1 h for adsorption. Cells were washed with PBS and
788 incubated for two additional hours at 37°C with media free of phenol red. Cells

789 were lysed using ONE-Glo EX Luciferase Assay System (Promega) and
790 luciferase activity was measured using EnSight Multimode Plate Reader
791 (PerkinElmer). Blocking assays were performed as follows: for antibody
792 blocking assay HeLa cells were incubated with two different concentrations of
793 anti-B2M antibody (5 and 15 µg/mL) or anti-caveolin antibody (15 µg/mL) -used
794 as negative control- 1 h at room temperature. Subsequently, the cells were
795 infected with V-e.luc (m.o.i.= 0.8) for 1 h and then washed with fresh medium.
796 After 3 h.p.i., cells were lysed and luciferase activity was measured. For B2M
797 blocking assay, V-e.luc inoculum was incubated with growing concentrations of
798 soluble BSA (control) or B2M (0, 5, 15, 30 and 50 µg/mL) 1 h at room
799 temperature. Then, HeLa cells were incubated with the pretreated inocula for 1h
800 and finally washed with fresh medium. At 3 h.p.i. cell extracts were prepared
801 and subsequently luciferase activity was measured.

802

803

804 **Immunofluorescence microscopy.**

805 Cells were seeded in round glass coverslips, washed with PBS, fixed with ice-
806 cold 4 % paraformaldehyde for 12 min and permeabilized in PBS containing 0.1
807 % Triton X-100 for 15 min at room-temperature. Cells were treated with PBS
808 containing 0.1 M glycine for 5 min and incubated with primary antibodies in
809 PBS-20 % FBS for 30 min, followed by incubation with secondary antibodies
810 diluted 1:300 in PBS-20 % FBS.

811 To detect virus particles by antibody labeling on the cell surface,
812 immunofluorescence was carried out on non-permeabilized cells treated as
813 follows: cells were seeded in coverslips, washed and incubated at 12 °C for 1 h

814 with primary antibodies in PBS-20 % FBS followed by incubation at 12 °C for 1
815 h with secondary antibodies in PBS-20 % FBS. Subsequently, cells were fixed
816 by ice-cold 4 % paraformaldehyde for 12 min and treated with PBS containing
817 0.1 M glycine for 5 min. Quantitation was derived from counting virus particles in
818 20-30 cells per sample.

819 Antibodies used were: Rabbit monoclonal anti-beta 2 Microglobulin EP2978Y
820 antibody (abcam, ref ab75853) diluted 1:300; Mouse monoclonal anti-Integrin
821 beta 1 [12G10] antibody (abcam, ref ab30394) diluted 1:70; Mouse monoclonal
822 anti-VAC (WR) A27L (Beiresources, ref: NR-569) diluted 1:250; anti-mouse
823 IgG-Alexa Fluor 488, anti-mouse IgG-Alexa Fluor 594, anti-rabbit IgG-Alexa
824 Fluor 488 antibodies (Invitrogen) diluted 1:300. Mouse monoclonal anti-Flag
825 1:500 (Sigma F1804).

826 For DNA staining, cells in glass coverslips were incubated with 2 mg/mL
827 bisbenzimidazole (Hoechst dye. Sigma) for 30 min. Cell surface staining was
828 performed by incubation with 0.02 mg/mL wheat germ agglutinin (WGA)-
829 Alexa488 (ThermoFisher Scientific) incubation at concentration for 30 min at 12
830 °C.

831 For internalization assay, cells were seeded in coverslips, and VV A4-cherry
832 (m.o.i. = 4) was incubated 1 h at 4°C to allow viral adsorption. Cells were then
833 incubated at 37°C for different times in a 5 % CO₂ incubator to allow
834 internalization. Cells were washed three times with PBS and incubated with
835 antibodies following the non-permeabilization method described above.

836 Binding assays were based on protocols described elsewhere (6, 20, 82, 83).
837 Briefly, cells grown in coverslips were infected with VV A4-cherry for 1 h at 4 °C
838 (m.o.i. = 30), washed with ice-cold PBS and fixated with paraformaldehyde 4 %

839 for 12 min at 4 °C. Cells were treated with PBS containing 0.1 M glycine for 5
840 min and incubated 30 min with 0.02 mg/mL Wheat Germ Agglutinin-Alexa488
841 diluted in PBS-20 % FBS. Cells were washed with PBS, mounted with
842 FluorSave reagent (Millipore) and observed by fluorescence microscopy.

843

844 **Western blotting.**

845 Whole cell lysates were prepared in denaturant buffer (80 mM Tris-HCl, pH 6.8,
846 2 % sodium dodecyl sulfate [SDS], 10 % glycerol, 0.01 % bromophenol blue
847 solution and 0.71 M 2-mercaptoethanol). After SDS-polyacrylamide gel
848 electrophoresis (PAGE), proteins were transferred to PVDF membranes and
849 incubated 1 h at RT with primary antibody in PBS containing 0.05 % Tween-20
850 and 1 % nonfat dry milk. Primary antibodies were Rabbit monoclonal anti-beta 2
851 Microglobulin EP2978Y antibody (abcam, ref ab75853) diluted 1:100; Rabbit
852 monoclonal anti-Axl C89E7 antibody (Cell Signaling Technology, ref 8661)
853 diluted 1:1000; Rabbit polyclonal anti-beta Actin antibody (GeneTex, ref
854 GTX109639) diluted 1:1000 and Mouse monoclonal anti-Flag 1:1000 (Sigma
855 F1804). After extensive washing with PBS-0.05 % Tween-20, membranes were
856 incubated with HRP-conjugated secondary antibodies diluted 1:3000.
857 Secondary antibodies were polyclonal goat anti-rabbit IgG (Dako P0448), and
858 anti-mouse polyvalent immunoglobulins (Sigma, ref: A0412). After removal of
859 unbound antibody, membranes were incubated for 1 min with a 1:1 mix of
860 solution A (2.5 mM luminol [Sigma], 0.4 mM p-coumaric acid [Sigma], 100 mM
861 Tris-HCl, pH 8.5) and solution B (0.018 % H₂O₂, 100 mM Tris-HCl, pH 8.5) to
862 finally record the luminiscence using a Molecular Imager Chemi Doc-XRS (Bio-
863 Rad).

864

865 **AKNOWLEDGEMENTS**

866 We are grateful to Dr. Wen Chang for plasmid pm-cherry-A4L and Jerson
867 Garita-Cambronero for assistance with computer analysis. Our gratitude to Dr.
868 Feng Zhang for making the CRISPR/Cas human pooled libraries available
869 through Addgene. We want to thank Marco Y. Hein for critical reading of the
870 manuscript. A.M. was recipient of a predoctoral contract from Subprograma
871 Estatal de Formación, Programa Estatal de Promoción del Talento y su
872 Empleabilidad en I+D+I, Spain.

873

874

875

876 REFERENCES

877

- 878 1. Moss B. Poxviridae: the viruses and their replication. *Fields Virology*. 2007;2:2905-46.
- 879 2. Howley PM, Knipe DM. *Fields virology*. 7th ed. Philadelphia: Wolters Kluwer; 2020.
- 880 3. Schmidt FI, Bleck CK, Mercer J. Poxvirus host cell entry. *Curr Opin Virol*. 2012;2(1):20-7.
- 881 4. Moss B. Poxvirus entry and membrane fusion. *Virology*. 2006;344(1):48-54.
- 882 5. Chiu WL, Lin CL, Yang MH, Tzou DL, Chang W. Vaccinia virus 4c (A26L) protein on
883 intracellular mature virus binds to the extracellular cellular matrix laminin. *J Virol*.
884 2007;81(5):2149-57.
- 885 6. Izmailyan R, Hsao JC, Chung CS, Chen CH, Hsu PW, Liao CL, et al. Integrin beta1
886 mediates vaccinia virus entry through activation of PI3K/Akt signaling. *J Virol*.
887 2012;86(12):6677-87.
- 888 7. Hiley CT, Chard LS, Gangeswaran R, Tysome JR, Briat A, Lemoine NR, et al. Vascular
889 endothelial growth factor A promotes vaccinia virus entry into host cells via activation of the
890 Akt pathway. *J Virol*. 2013;87(5):2781-90.
- 891 8. Morizono K, Xie Y, Olafsen T, Lee B, Dasgupta A, Wu AM, et al. The soluble serum
892 protein Gas6 bridges virion envelope phosphatidylserine to the TAM receptor tyrosine kinase
893 Axl to mediate viral entry. *Cell Host Microbe*. 2011;9(4):286-98.
- 894 9. Rizopoulos Z, Balistreri G, Kilcher S, Martin CK, Syedbasha M, Helenius A, et al. Vaccinia
895 Virus Infection Requires Maturation of Macropinosomes. *Traffic*. 2015;16(8):814-31.
- 896 10. Schmidt FI, Bleck CK, Helenius A, Mercer J. Vaccinia extracellular virions enter cells by
897 macropinocytosis and acid-activated membrane rupture. *EMBO J*. 2011;30(17):3647-61.
- 898 11. Townsley AC, Weisberg AS, Wagenaar TR, Moss B. Vaccinia virus entry into cells via a
899 low-pH-dependent endosomal pathway. *J Virol*. 2006;80(18):8899-908.
- 900 12. Mercer J, Helenius A. Vaccinia virus uses macropinocytosis and apoptotic mimicry to
901 enter host cells. *Science*. 2008;320(5875):531-5.
- 902 13. Mercer J, Helenius A. Apoptotic mimicry: phosphatidylserine-mediated
903 macropinocytosis of vaccinia virus. *Ann N Y Acad Sci*. 2010;1209:49-55.
- 904 14. Moss B. Membrane fusion during poxvirus entry. *Semin Cell Dev Biol*. 2016;60:89-96.
- 905 15. Bengali Z, Satheshkumar PS, Moss B. Orthopoxvirus species and strain differences in
906 cell entry. *Virology*. 2012;433(2):506-12.
- 907 16. Bengali Z, Townsley AC, Moss B. Vaccinia virus strain differences in cell attachment and
908 entry. *Virology*. 2009;389(1-2):132-40.
- 909 17. Carter GC, Law M, Hollinshead M, Smith GL. Entry of the vaccinia virus intracellular
910 mature virion and its interactions with glycosaminoglycans. *J Gen Virol*. 2005;86(Pt 5):1279-90.
- 911 18. Mercer J, Knebel S, Schmidt FI, Crouse J, Burkard C, Helenius A. Vaccinia virus strains
912 use distinct forms of macropinocytosis for host-cell entry. *Proc Natl Acad Sci U S A*.
913 2010;107(20):9346-51.
- 914 19. Locker JK, Kuehn A, Schleich S, Rutter G, Hohenberg H, Wepf R, et al. Entry of the two
915 infectious forms of vaccinia virus at the plasma membrane is signaling-dependent for the IMV
916 but not the EEV. *Mol Biol Cell*. 2000;11(7):2497-511.
- 917 20. Vanderplasschen A, Hollinshead M, Smith GL. Intracellular and extracellular vaccinia
918 virions enter cells by different mechanisms. *J Gen Virol*. 1998;79 (Pt 4):877-87.
- 919 21. Ma H, Dang Y, Wu Y, Jia G, Anaya E, Zhang J, et al. A CRISPR-Based Screen Identifies
920 Genes Essential for West-Nile-Virus-Induced Cell Death. *Cell Rep*. 2015;12(4):673-83.
- 921 22. Li B, Clohisey SM, Chia BS, Wang B, Cui A, Eisenhaure T, et al. Genome-wide CRISPR
922 screen identifies host dependency factors for influenza A virus infection. *Nat Commun*.
923 2020;11(1):164.

- 924 23. Li Y, Muffat J, Omer Javed A, Keys HR, Lungjangwa T, Bosch I, et al. Genome-wide
925 CRISPR screen for Zika virus resistance in human neural cells. *Proc Natl Acad Sci U S A*.
926 2019;116(19):9527-32.
- 927 24. Zhu Y, Feng F, Hu G, Wang Y, Yu Y, Zhu Y, et al. A genome-wide CRISPR screen identifies
928 host factors that regulate SARS-CoV-2 entry. *Nat Commun*. 2021;12(1):961.
- 929 25. Hein MY, Weissman JS. Functional single-cell genomics of human cytomegalovirus
930 infection. *Nat Biotechnol*. 2022;40(3):391-401.
- 931 26. Wei J, Alfajaro MM, DeWeirdt PC, Hanna RE, Lu-Culligan WJ, Cai WL, et al. Genome-
932 wide CRISPR Screens Reveal Host Factors Critical for SARS-CoV-2 Infection. *Cell*.
933 2021;184(1):76-91 e13.
- 934 27. Moser TS, Jones RG, Thompson CB, Coyne CB, Cherry S. A kinome RNAi screen
935 identified AMPK as promoting poxvirus entry through the control of actin dynamics. *PLoS*
936 *Pathog*. 2010;6(6):e1000954.
- 937 28. Mercer J, Snijder B, Sacher R, Burkard C, Bleck CK, Stahlberg H, et al. RNAi screening
938 reveals proteasome- and Cullin3-dependent stages in vaccinia virus infection. *Cell Rep*.
939 2012;2(4):1036-47.
- 940 29. Sivan G, Martin SE, Myers TG, Buehler E, Szymczyk KH, Ormanoglu P, et al. Human
941 genome-wide RNAi screen reveals a role for nuclear pore proteins in poxvirus morphogenesis.
942 *Proc Natl Acad Sci U S A*. 2013;110(9):3519-24.
- 943 30. Beard PM, Griffiths SJ, Gonzalez O, Haga IR, Pechenick Jowers T, Reynolds DK, et al. A
944 loss of function analysis of host factors influencing Vaccinia virus replication by RNA
945 interference. *PLoS One*. 2014;9(6):e98431.
- 946 31. Realegeno S, Puschnik AS, Kumar A, Goldsmith C, Burgado J, Sambhara S, et al.
947 Monkeypox Virus Host Factor Screen Using Haploid Cells Identifies Essential Role of GARP
948 Complex in Extracellular Virus Formation. *J Virol*. 2017;91(11).
- 949 32. Luteijn RD, van Diemen F, Blomen VA, Boer IGJ, Manikam Sadasivam S, van Kuppevelt
950 TH, et al. A Genome-Wide Haploid Genetic Screen Identifies Heparan Sulfate-Associated Genes
951 and the Macropinocytosis Modulator TMED10 as Factors Supporting Vaccinia Virus Infection. *J*
952 *Virol*. 2019;93(13).
- 953 33. Sanjana NE, Shalem O, Zhang F. Improved vectors and genome-wide libraries for
954 CRISPR screening. *Nat Methods*. 2014;11(8):783-4.
- 955 34. Shalem O, Sanjana NE, Hartenian E, Shi X, Scott DA, Mikkelsen T, et al. Genome-scale
956 CRISPR-Cas9 knockout screening in human cells. *Science*. 2014;343(6166):84-7.
- 957 35. Krangel MS, Orr HT, Strominger JL. Assembly and maturation of HLA-A and HLA-B
958 antigens in vivo. *Cell*. 1979;18(4):979-91.
- 959 36. Feder JN, Gnirke A, Thomas W, Tsuchihashi Z, Ruddy DA, Basava A, et al. A novel MHC
960 class I-like gene is mutated in patients with hereditary haemochromatosis. *Nat Genet*.
961 1996;13(4):399-408.
- 962 37. Praetor A, Hunziker W. beta(2)-Microglobulin is important for cell surface expression
963 and pH-dependent IgG binding of human FcRn. *J Cell Sci*. 2002;115(Pt 11):2389-97.
- 964 38. Yamaguchi H, Hashimoto K. Association of MR1 protein, an MHC class I-related
965 molecule, with beta(2)-microglobulin. *Biochem Biophys Res Commun*. 2002;290(2):722-9.
- 966 39. Wang T, Birsoy K, Hughes NW, Krupczak KM, Post Y, Wei JJ, et al. Identification and
967 characterization of essential genes in the human genome. *Science*. 2015;350(6264):1096-101.
- 968 40. Bertomeu T, Coulombe-Huntington J, Chatr-Aryamontri A, Bourdages KG, Coyaud E,
969 Raught B, et al. A High-Resolution Genome-Wide CRISPR/Cas9 Viability Screen Reveals
970 Structural Features and Contextual Diversity of the Human Cell-Essential Proteome. *Mol Cell*
971 *Biol*. 2018;38(1).
- 972 41. Lorenzo MM, Sanchez-Puig JM, Blasco R. Genes A27L and F13L as Genetic Markers for
973 the Isolation of Recombinant Vaccinia Virus. *Sci Rep*. 2019;9(1):15684.

- 974 42. Sanderson CM, Hollinshead M, Smith GL. The vaccinia virus A27L protein is needed for
975 the microtubule-dependent transport of intracellular mature virus particles. *J Gen Virol*.
976 2000;81(Pt 1):47-58.
- 977 43. Holzer GW, Falkner FG. Construction of a vaccinia virus deficient in the essential DNA
978 repair enzyme uracil DNA glycosylase by a complementing cell line. *J Virol*. 1997;71(7):4997-
979 5002.
- 980 44. Ricci PS, Schafer B, Kreil TR, Falkner FG, Holzer GW. Selection of recombinant MVA by
981 rescue of the essential D4R gene. *Virology*. 2011;8:529.
- 982 45. Li W, Xu H, Xiao T, Cong L, Love MI, Zhang F, et al. MAGECK enables robust
983 identification of essential genes from genome-scale CRISPR/Cas9 knockout screens. *Genome*
984 *Biol*. 2014;15(12):554.
- 985 46. Wang B, Wang M, Zhang W, Xiao T, Chen CH, Wu A, et al. Integrative analysis of pooled
986 CRISPR genetic screens using MAGECKFlute. *Nat Protoc*. 2019;14(3):756-80.
- 987 47. Meyers RM, Bryan JG, McFarland JM, Weir BA, Sizemore AE, Xu H, et al. Computational
988 correction of copy number effect improves specificity of CRISPR-Cas9 essentiality screens in
989 cancer cells. *Nat Genet*. 2017;49(12):1779-84.
- 990 48. Yu J, Silva J, Califano A. ScreenBEAM: a novel meta-analysis algorithm for functional
991 genomics screens via Bayesian hierarchical modeling. *Bioinformatics*. 2016;32(2):260-7.
- 992 49. Grimbert P, Valanciute A, Audard V, Lang P, Guellaen G, Sahali D. The Filamin-A is a
993 partner of Tc-mip, a new adapter protein involved in c-maf-dependent Th2 signaling pathway.
994 *Mol Immunol*. 2004;40(17):1257-61.
- 995 50. Grimbert P, Valanciute A, Audard V, Pawlak A, Le gouvelo S, Lang P, et al. Truncation of
996 C-mip (Tc-mip), a new proximal signaling protein, induces c-maf Th2 transcription factor and
997 cytoskeleton reorganization. *J Exp Med*. 2003;198(5):797-807.
- 998 51. Rintala-Dempsey AC, Rezvanpour A, Shaw GS. S100-annexin complexes--structural
999 insights. *FEBS J*. 2008;275(20):4956-66.
- 1000 52. Liu Y, Myrvang HK, Dekker LV. Annexin A2 complexes with S100 proteins: structure,
1001 function and pharmacological manipulation. *Br J Pharmacol*. 2015;172(7):1664-76.
- 1002 53. Canales J, Cruz P, Diaz N, Riquelme D, Leiva-Salcedo E, Cerda O. K(+) Channel
1003 Tetramerization Domain 5 (KCTD5) Protein Regulates Cell Migration, Focal Adhesion Dynamics
1004 and Spreading through Modulation of Ca(2+) Signaling and Rac1 Activity. *Cells*. 2020;9(10).
- 1005 54. Bayon Y, Trinidad AG, de la Puerta ML, Del Carmen Rodriguez M, Bogetz J, Rojas A, et
1006 al. KCTD5, a putative substrate adaptor for cullin3 ubiquitin ligases. *FEBS J*. 2008;275(15):3900-
1007 10.
- 1008 55. Yu G, He QY. ReactomePA: an R/Bioconductor package for reactome pathway analysis
1009 and visualization. *Mol Biosyst*. 2016;12(2):477-9.
- 1010 56. Spriggs MK, Koller BH, Sato T, Morrissey PJ, Fanslow WC, Smithies O, et al. Beta 2-
1011 microglobulin-, CD8+ T-cell-deficient mice survive inoculation with high doses of vaccinia virus
1012 and exhibit altered IgG responses. *Proc Natl Acad Sci U S A*. 1992;89(13):6070-4.
- 1013 57. Epstein SL, Mispion JA, Lawson CM, Subbarao EK, Connors M, Murphy BR. Beta 2-
1014 microglobulin-deficient mice can be protected against influenza A infection by vaccination with
1015 vaccinia-influenza recombinants expressing hemagglutinin and neuraminidase. *J Immunol*.
1016 1993;150(12):5484-93.
- 1017 58. Laliberte JP, Weisberg AS, Moss B. The membrane fusion step of vaccinia virus entry is
1018 cooperatively mediated by multiple viral proteins and host cell components. *PLoS Pathog*.
1019 2011;7(12):e1002446.
- 1020 59. Laliberte JP, Moss B. Appraising the apoptotic mimicry model and the role of
1021 phospholipids for poxvirus entry. *Proc Natl Acad Sci U S A*. 2009;106(41):17517-21.
- 1022 60. Thul PJ, Akesson L, Wiking M, Mahdessian D, Geladaki A, Ait Blal H, et al. A subcellular
1023 map of the human proteome. *Science*. 2017;356(6340).
- 1024 61. Moller-Tank S, Maury W. Phosphatidylserine receptors: enhancers of enveloped virus
1025 entry and infection. *Virology*. 2014;468-470:565-80.

- 1026 62. Schroeder N, Chung CS, Chen CH, Liao CL, Chang W. The lipid raft-associated protein
1027 CD98 is required for vaccinia virus endocytosis. *J Virol.* 2012;86(9):4868-82.
- 1028 63. Gray RDM, Albrecht D, Beerli C, Huttunen M, Cohen GH, White IJ, et al. Nanoscale
1029 polarization of the entry fusion complex of vaccinia virus drives efficient fusion. *Nat Microbiol.*
1030 2019;4(10):1636-44.
- 1031 64. Ramsey-Ewing A, Moss B. Apoptosis induced by a postbinding step of vaccinia virus
1032 entry into Chinese hamster ovary cells. *Virology.* 1998;242(1):138-49.
- 1033 65. Velling T, Nilsson S, Stefansson A, Johansson S. beta1-Integrins induce phosphorylation
1034 of Akt on serine 473 independently of focal adhesion kinase and Src family kinases. *EMBO Rep.*
1035 2004;5(9):901-5.
- 1036 66. Gay CM, Balaji K, Byers LA. Giving AXL the axe: targeting AXL in human malignancy. *Br J*
1037 *Cancer.* 2017;116(4):415-23.
- 1038 67. Mattila PK, Lappalainen P. Filopodia: molecular architecture and cellular functions. *Nat*
1039 *Rev Mol Cell Biol.* 2008;9(6):446-54.
- 1040 68. Manni S, Carrino M, Semenzato G, Piazza F. Old and Young Actors Playing Novel Roles
1041 in the Drama of Multiple Myeloma Bone Marrow Microenvironment Dependent Drug
1042 Resistance. *Int J Mol Sci.* 2018;19(5).
- 1043 69. Apetoh L, Quintana FJ, Pot C, Joller N, Xiao S, Kumar D, et al. The aryl hydrocarbon
1044 receptor interacts with c-Maf to promote the differentiation of type 1 regulatory T cells
1045 induced by IL-27. *Nat Immunol.* 2010;11(9):854-61.
- 1046 70. Pot C. Aryl hydrocarbon receptor controls regulatory CD4+ T cell function. *Swiss Med*
1047 *Wkly.* 2012;142:w13592.
- 1048 71. Ollero M, Sahali D. The Enigmatic Emerging Role of the C-Maf Inducing Protein in
1049 Cancer. *Diagnostics (Basel).* 2021;11(4).
- 1050 72. Monteiro P, Gilot D, Le Ferrec E, Lecureur V, N'Diaye M, Le Vee M, et al. AhR- and c-
1051 maf-dependent induction of beta7-integrin expression in human macrophages in response to
1052 environmental polycyclic aromatic hydrocarbons. *Biochem Biophys Res Commun.*
1053 2007;358(2):442-8.
- 1054 73. Triantafilou M, Triantafilou K, Wilson KM, Takada Y, Fernandez N, Stanway G.
1055 Involvement of beta2-microglobulin and integrin alphavbeta3 molecules in the coxsackievirus
1056 A9 infectious cycle. *J Gen Virol.* 1999;80 (Pt 10):2591-600.
- 1057 74. Heikkila O, Susi P, Tevaluoto T, Harma H, Marjomaki V, Hyypia T, et al. Internalization
1058 of coxsackievirus A9 is mediated by {beta}2-microglobulin, dynamin, and Arf6 but not by
1059 caveolin-1 or clathrin. *J Virol.* 2010;84(7):3666-81.
- 1060 75. Heikkila O, Merilahti P, Hakanen M, Karelehto E, Alanko J, Sukki M, et al. Integrins are
1061 not essential for entry of coxsackievirus A9 into SW480 human colon adenocarcinoma cells.
1062 *Virol J.* 2016;13(1):171.
- 1063 76. Huang CY, Lu TY, Bair CH, Chang YS, Jwo JK, Chang W. A novel cellular protein, VPEF,
1064 facilitates vaccinia virus penetration into HeLa cells through fluid phase endocytosis. *J Virol.*
1065 2008;82(16):7988-99.
- 1066 77. Zhao X, Zhang G, Liu S, Chen X, Peng R, Dai L, et al. Human Neonatal Fc Receptor Is the
1067 Cellular Uncoating Receptor for Enterovirus B. *Cell.* 2019;177(6):1553-65 e16.
- 1068 78. Morosky S, Wells AI, Lemon K, Evans AS, Schamus S, Bakkenist CJ, et al. The neonatal
1069 Fc receptor is a pan-echovirus receptor. *Proc Natl Acad Sci U S A.* 2019;116(9):3758-63.
- 1070 79. Randazzo PA, Andrade J, Miura K, Brown MT, Long YQ, Stauffer S, et al. The Arf
1071 GTPase-activating protein ASAP1 regulates the actin cytoskeleton. *Proc Natl Acad Sci U S A.*
1072 2000;97(8):4011-6.
- 1073 80. Lorenzo MM, Galindo I, Blasco R. Construction and isolation of recombinant vaccinia
1074 virus using genetic markers. *Methods Mol Biol.* 2004;269:15-30.
- 1075 81. Earl PL, Cooper N, Wyatt LS, Moss B, Carroll MW. Preparation of cell cultures and
1076 vaccinia virus stocks. *Curr Protoc Mol Biol.* 2001;Chapter 16:Unit16

- 1077 82. Bisht H, Weisberg AS, Moss B. Vaccinia virus I1 protein is required for cell entry and
1078 membrane fusion. *J Virol.* 2008;82(17):8687-94.
1079 83. Vanderplasschen A, Smith GL. A novel virus binding assay using confocal microscopy:
1080 demonstration that the intracellular and extracellular vaccinia virions bind to different cellular
1081 receptors. *J Virol.* 1997;71(5):4032-41.

1082

1083

1084

1085 **Supporting information**

1086

1087 **S1 Fig. Screening experiment example.** A representative hit analysis for one
1088 of the 27 screen experiments analyzed with MaGeCK. For each gene, the LFC
1089 values from infected and non-infected cultures are represented. Gene hits with
1090 FDR < 0.05 that also show LFC > 0 in infected and LFC < 0 in non-infected are
1091 labeled with gene name tags. Best hits are those that have the greatest LFC in
1092 infected control and the lowest LFC in control experiments (non infected). Note
1093 that genes with non infected LFC > 1 could be positive hits as well.

1094

1095 **S2 Fig. VV / B2M colocalization rates.** HeLa cells were infected with VV A4-
1096 cherry (red) for 1 h at 4 °C and unbound virus was removed by washing (m.o.i.
1097 = 5). Non-permeabilized cells were then incubated for different times at 37 °C
1098 and stained with anti-B2M to analyze colocalization.

1099

1100 **S3 Fig. Blocking assay for VV entry by soluble B2M.** V-e.luc virus was
1101 incubated with increasing concentrations of soluble BSA (control) or B2M (0, 5,
1102 15, 30 and 50 µg/mL) protein for 1 h at room temperature. Then, HeLa cells
1103 were incubated for 1 h with the pre-treated inoculum. At 3 h.p.i. luciferase
1104 activity was determined as a measure of viral entry and early gene expression.
1105 No significant differences were found. p-values: **** < 0.0001, *** < 0.001, ** <
1106 0.01, * < 0.05, ns > 0.05.

1107

1108 **S4 Fig. Blocking assay for VV entry with anti-B2M antibody.** HeLa cells
1109 were incubated with two different concentrations of anti-B2M antibody (5 and 15
1110 $\mu\text{g}/\text{mL}$) for 1 h at room temperature. Anti-caveolin antibody (15 $\mu\text{g}/\text{mL}$) was
1111 used as negative control. After antibody treatment, HeLa cells were infected
1112 with V-e.luc (m.o.i. 0.8), and eventually 3 h.p.i. luciferase activity was
1113 determined as a measure of viral entry and early gene expression. No
1114 significant differences were found. ns, not significant ($p > 0.05$).

1115

1116 **S1 Table. Screen_conditions.** Different screen experiments were performed.
1117 Experiments are summarized where which mutant, m.o.i. and number of
1118 reinfections is showed.

1119

1120 **S2 Table. Screen Results.** Gene summary files obtained from MaGeCK test
1121 showing the FDR and LFC for each gene in each experiment.

1122

1123 **S3 Table. ScreenBEAMresults.** Summary of ScreenBEAM results showing
1124 good guides, B-score, z-score, p-value, FDR and standard deviations for each
1125 gene, where x is for control experiment and y for infected experiment. Top 20
1126 genes were selected as hits.

1127

1128 **S4 Table. Reactome_Pathway analysis.** Results from Reactome Pathway
1129 analysis. The most enriched pathways are shown in descendent order.
1130 Statistical data is shown (i.e. pvalue, p.adjust), as well as the genes ID that
1131 belong to each enriched pathway.

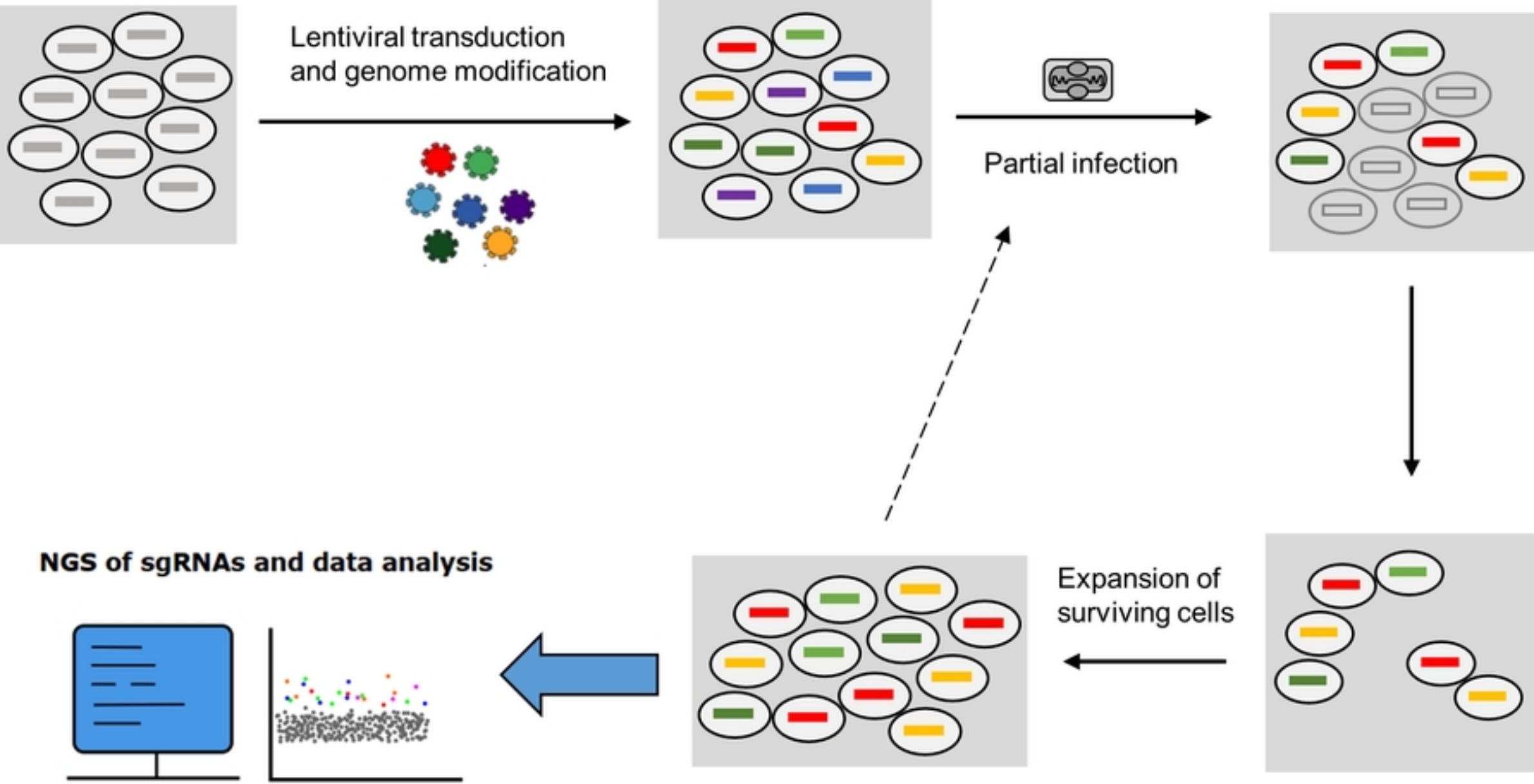


Figure 1

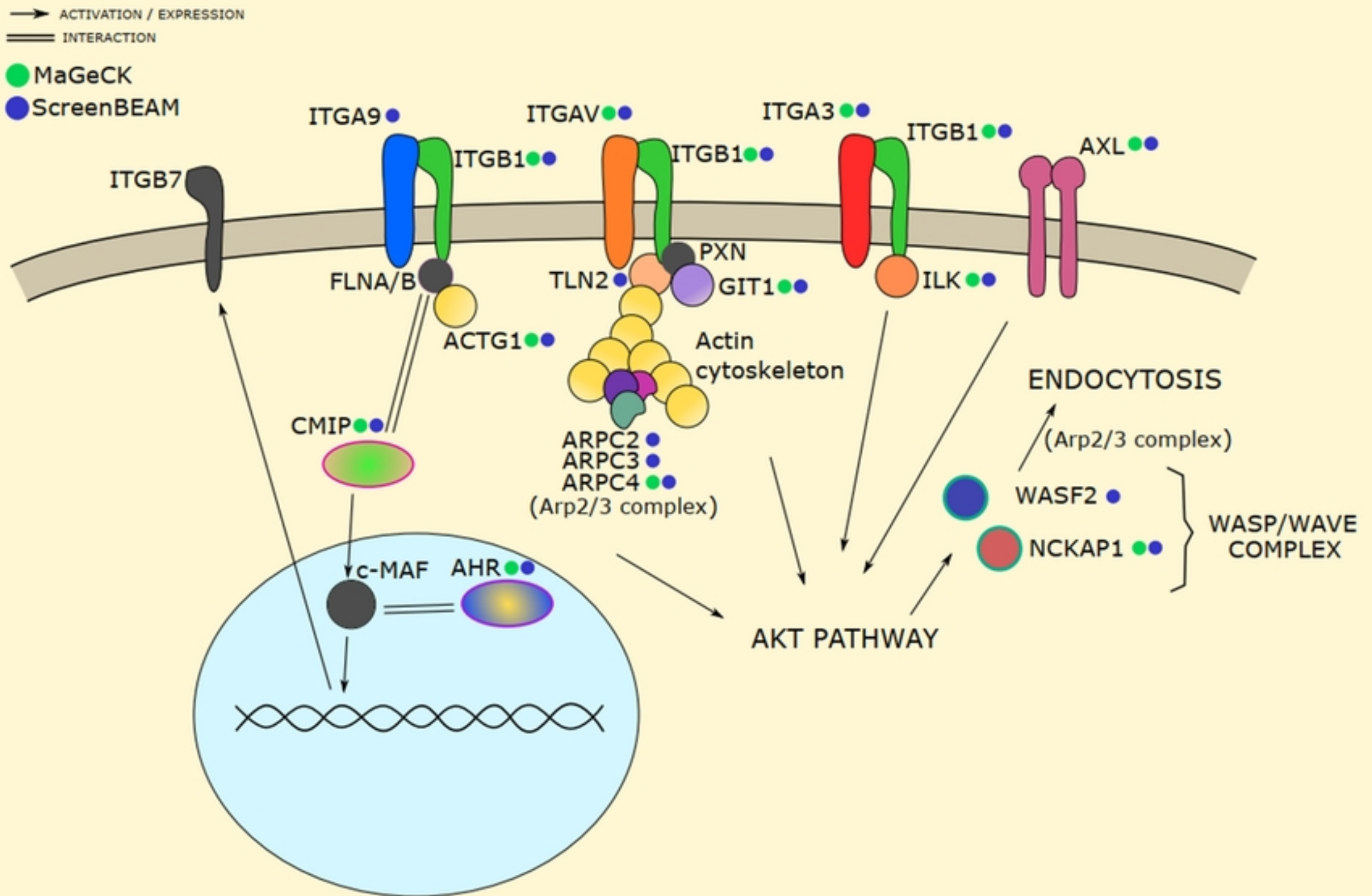


Figure 3

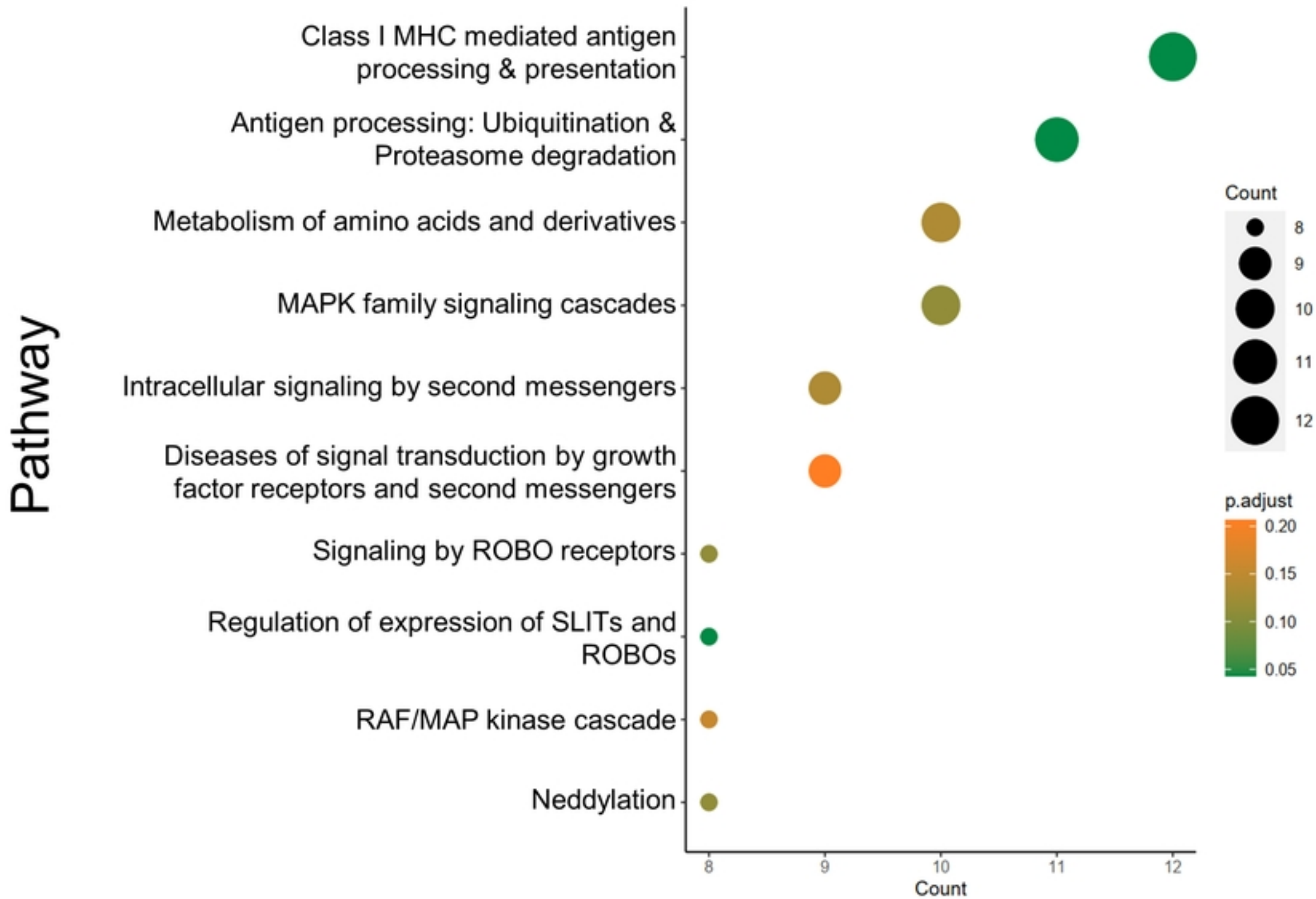


Figure 4

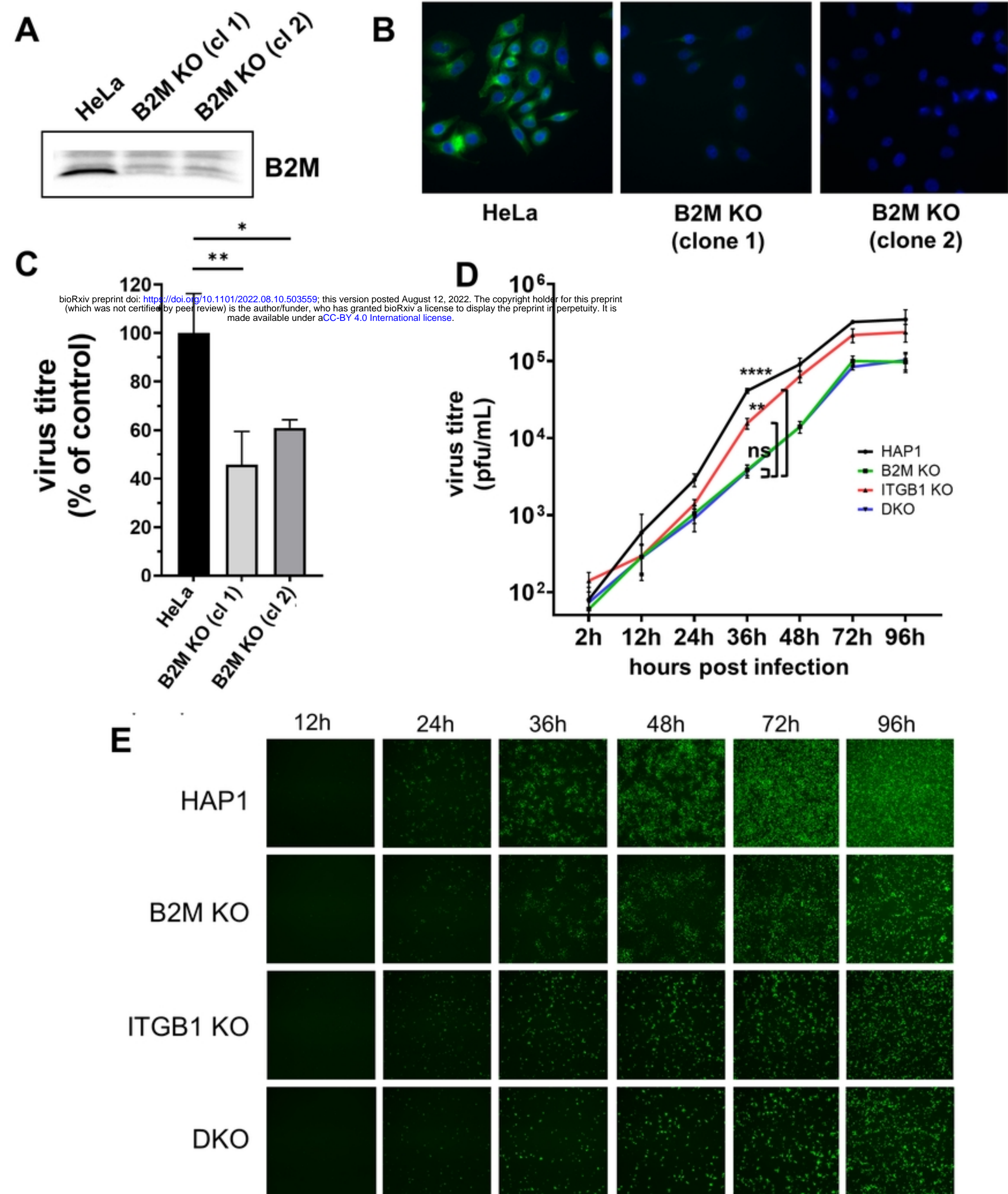


Figure 5

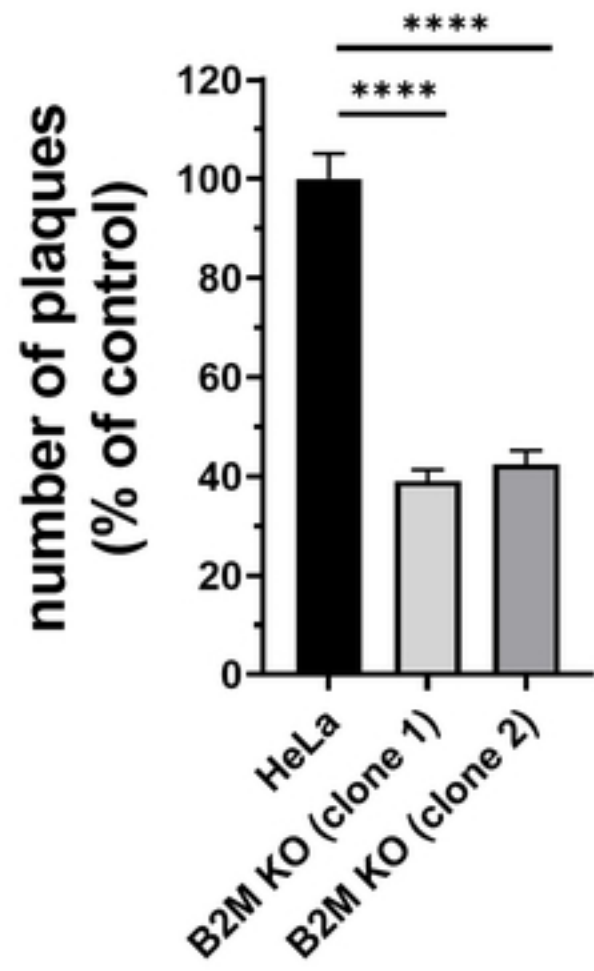
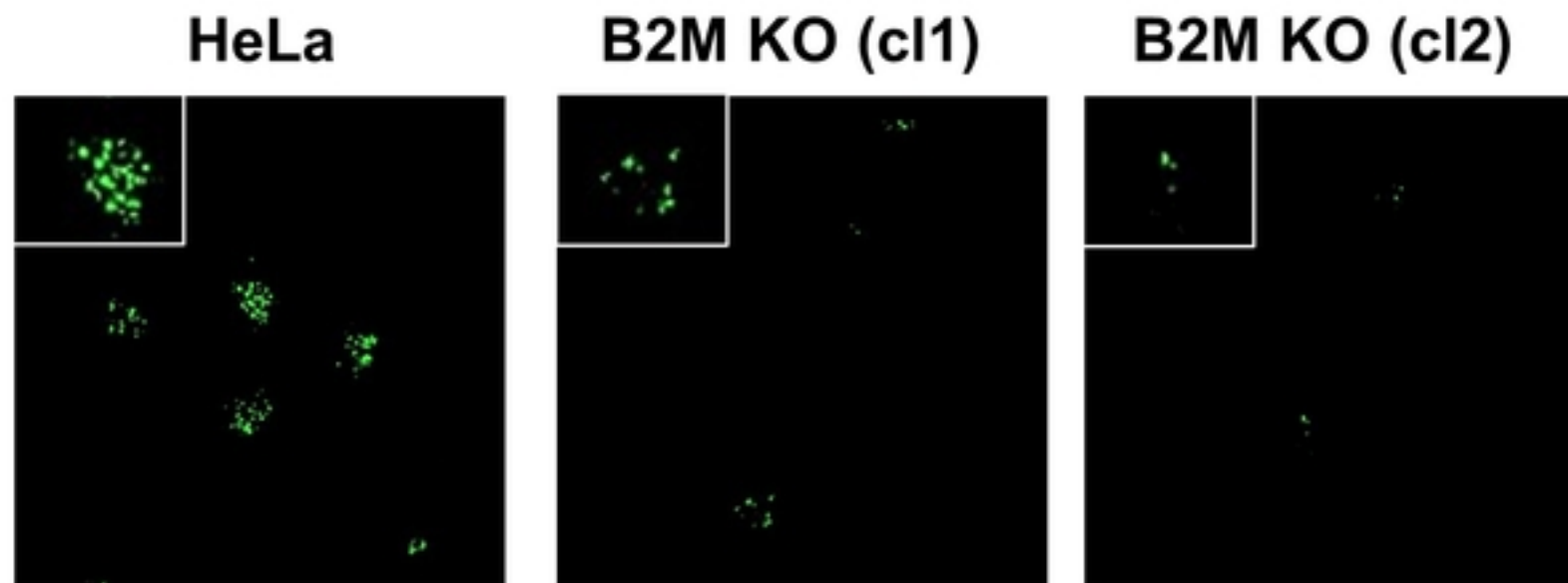
A**B**

Figure 6

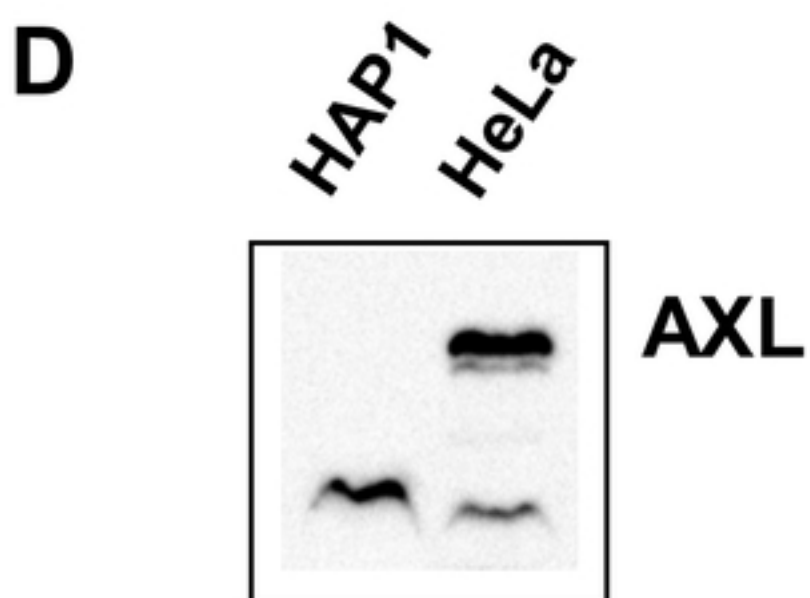
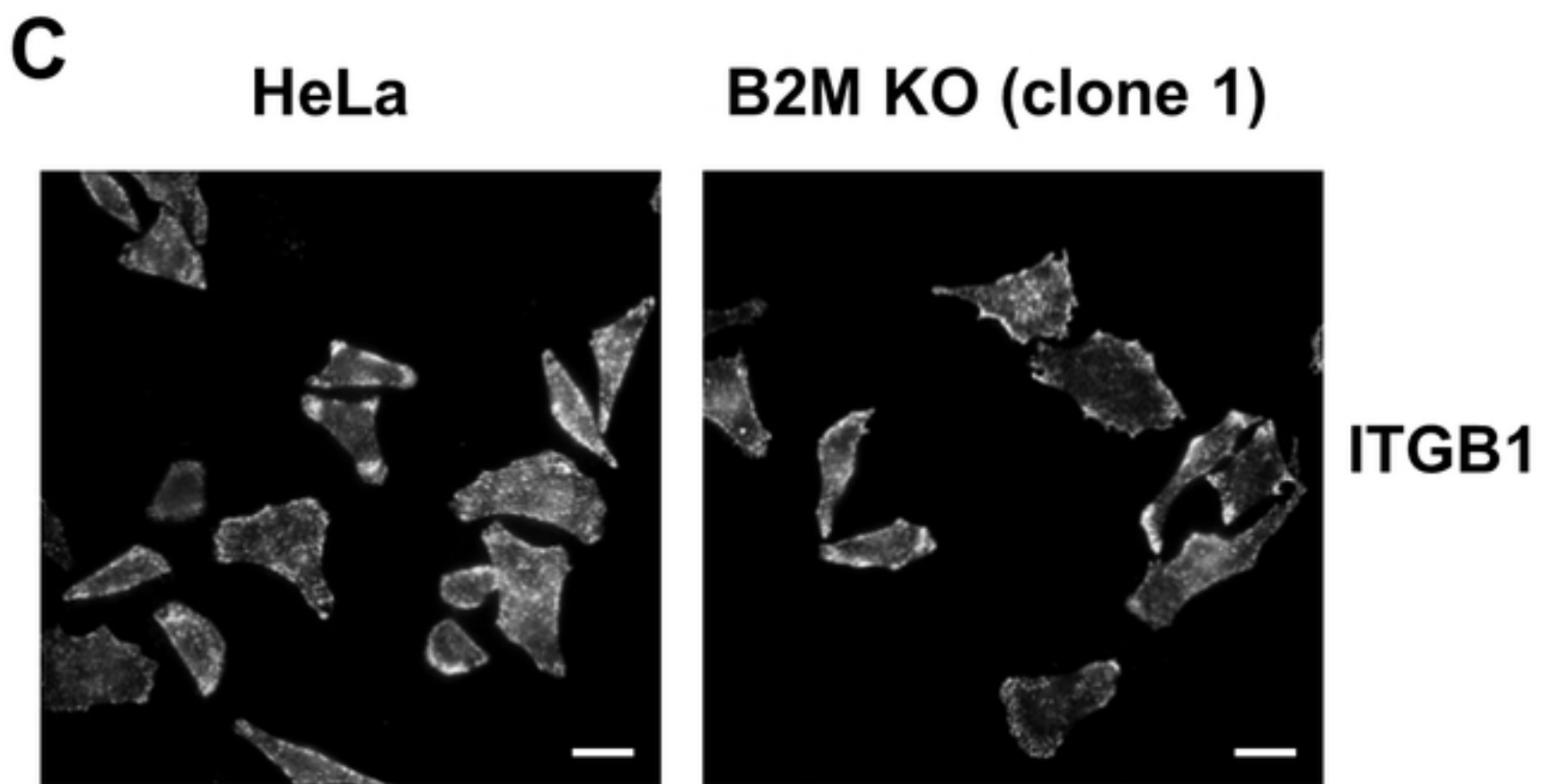
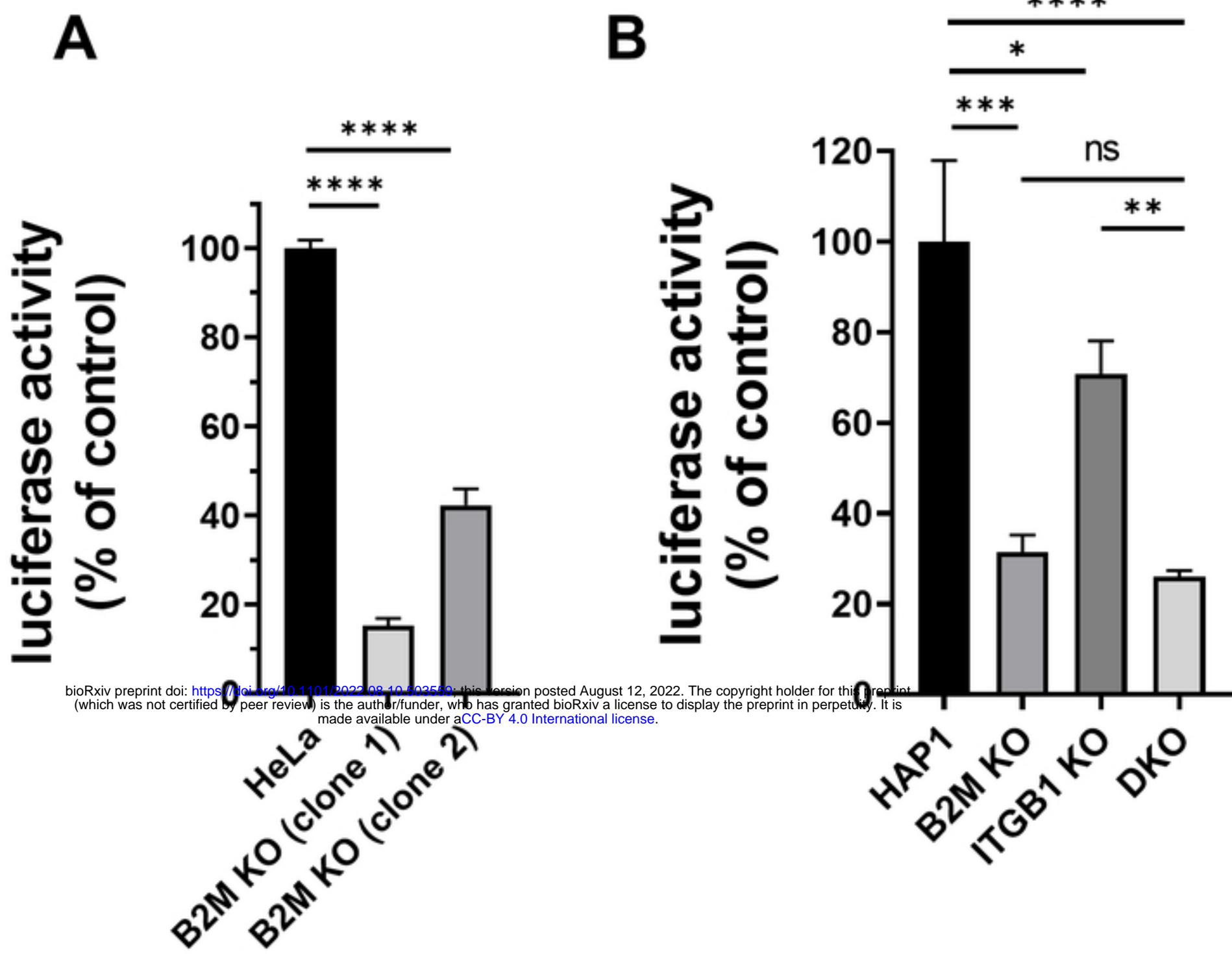


Figure 7

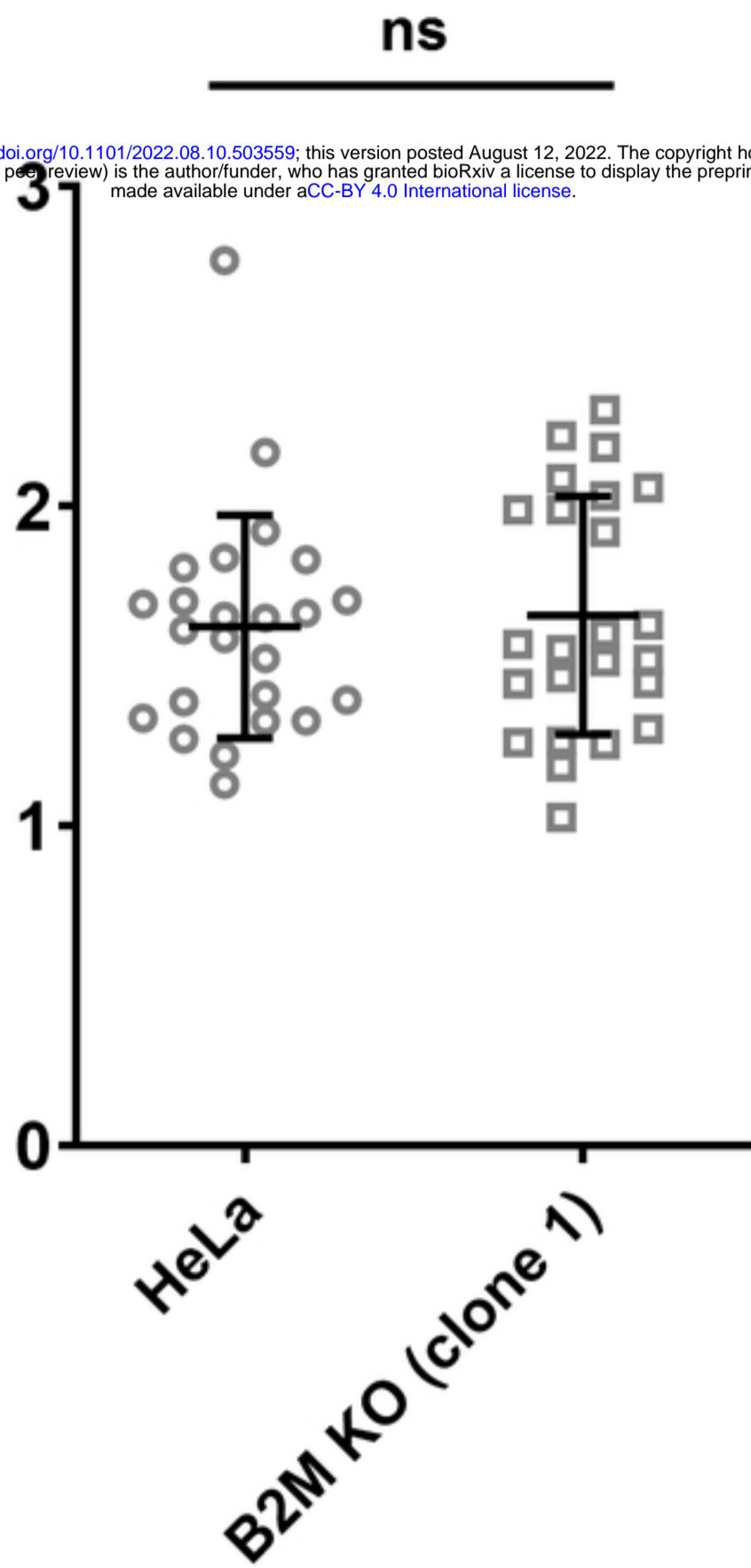
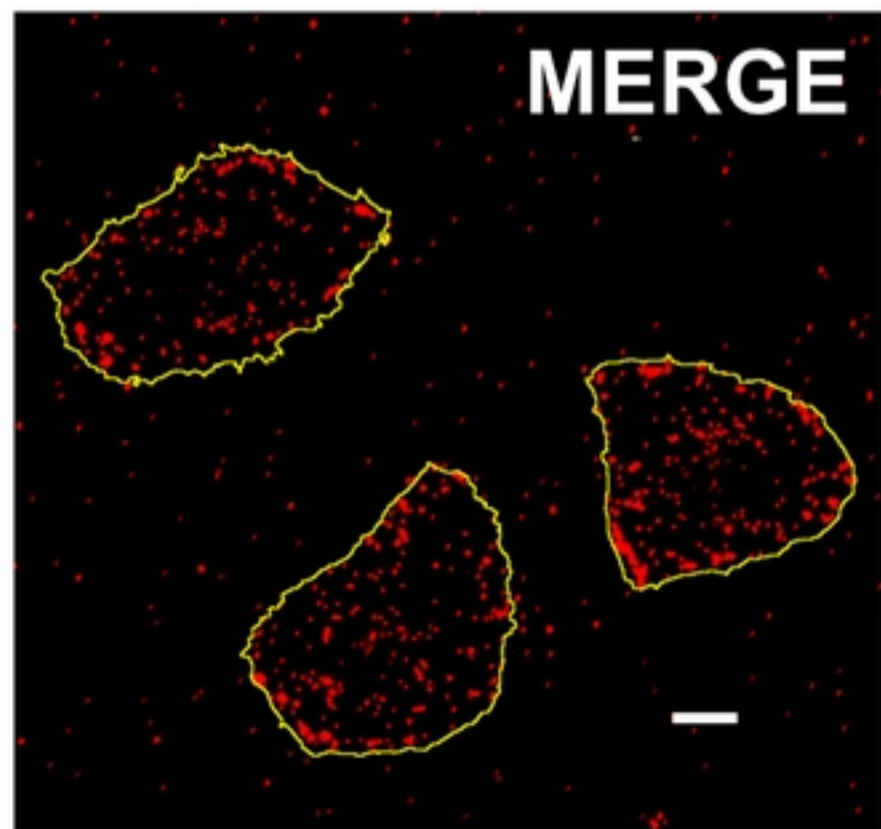
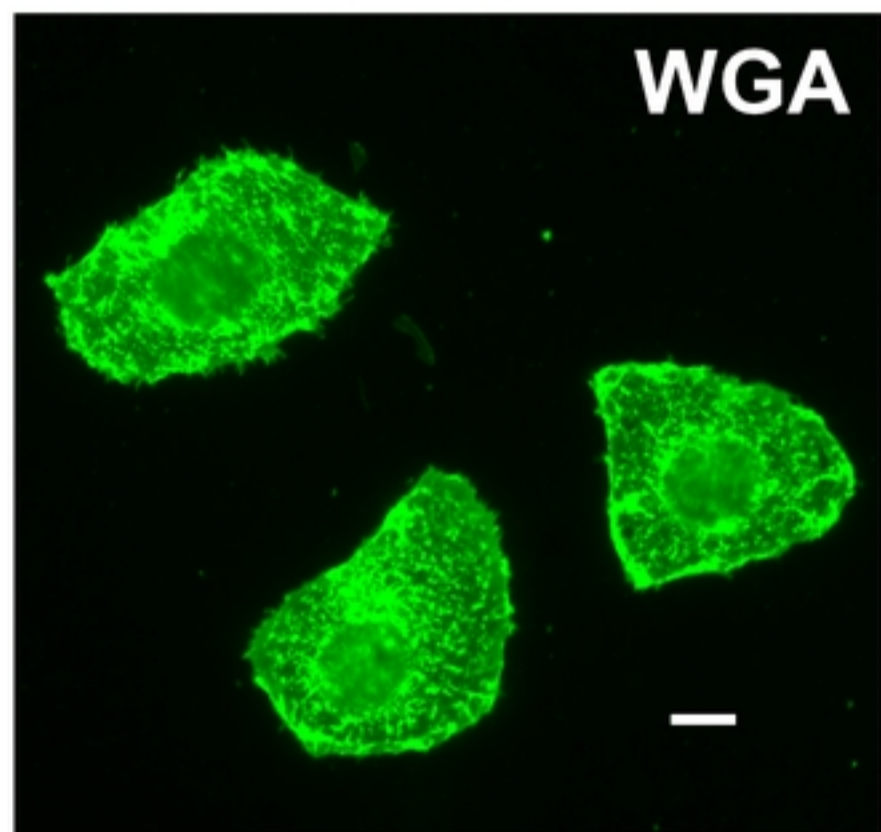
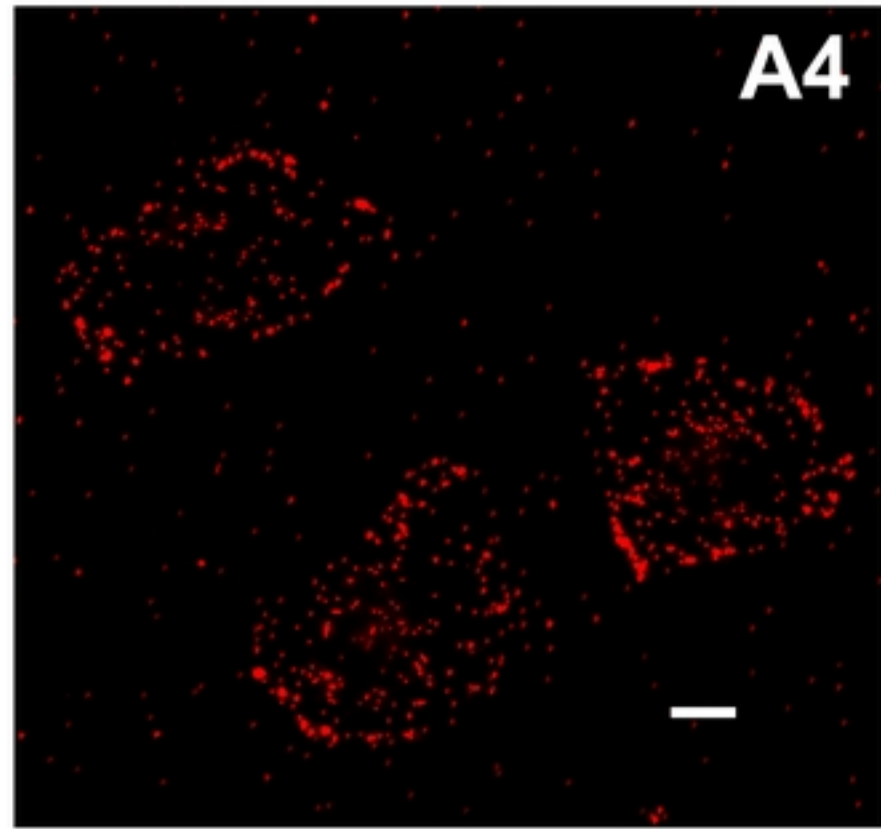
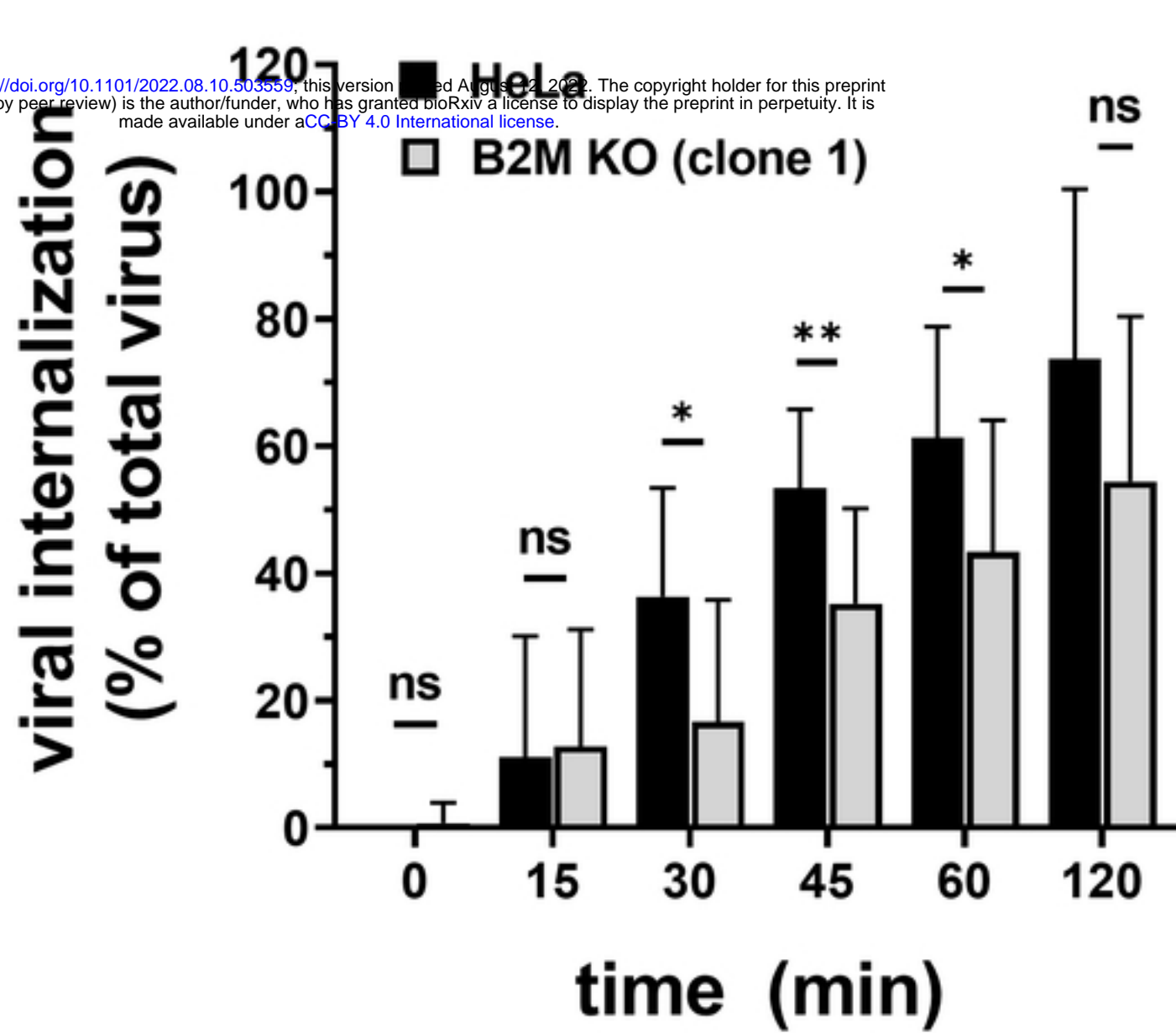
A**viral binding
(particles/surface x1000)****B**

Figure 8



B

A4

A27

MERGE

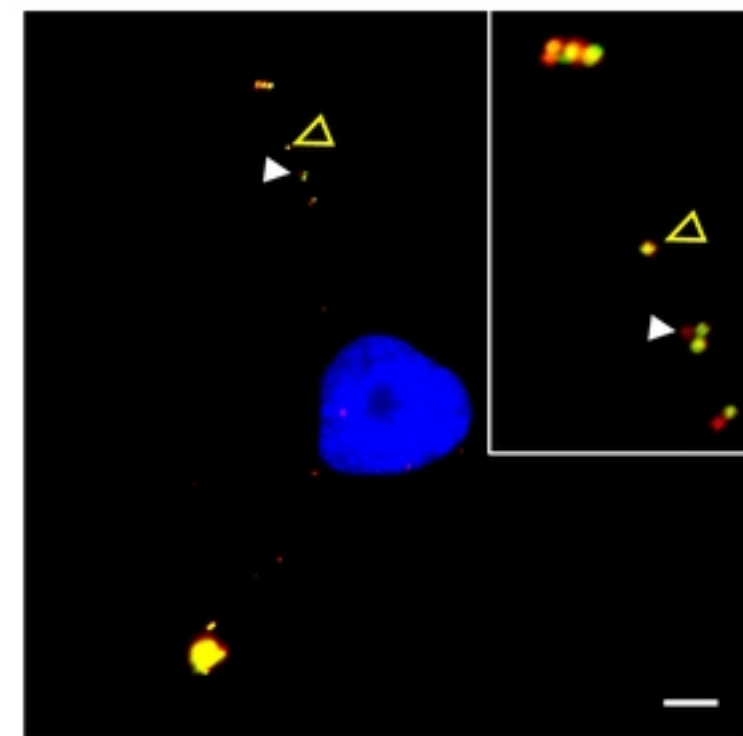
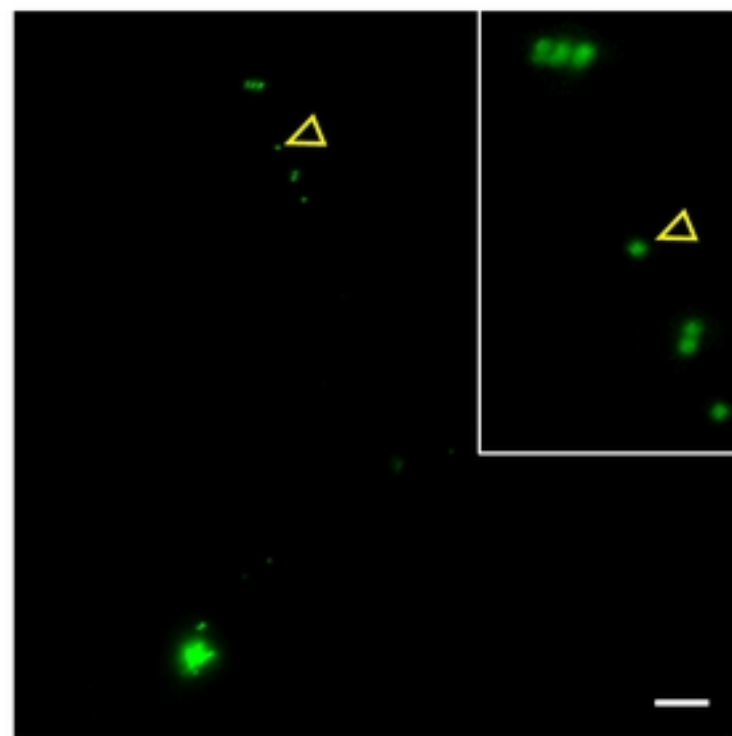
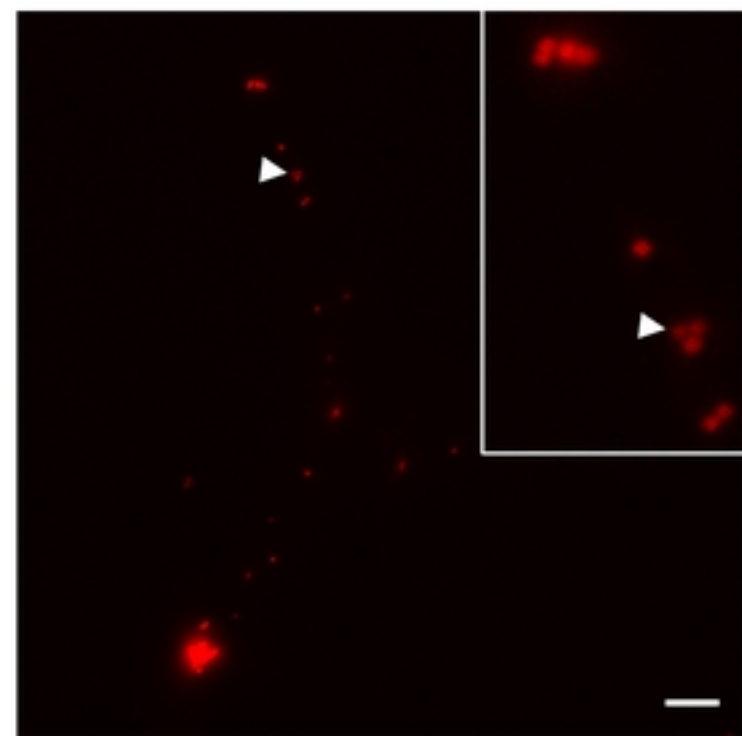


Figure 9

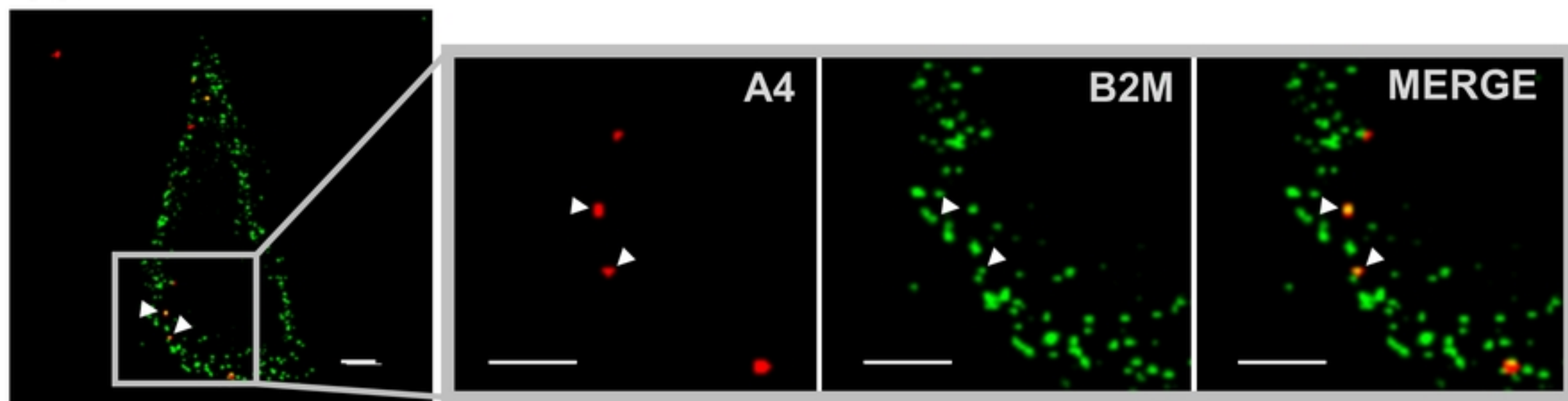
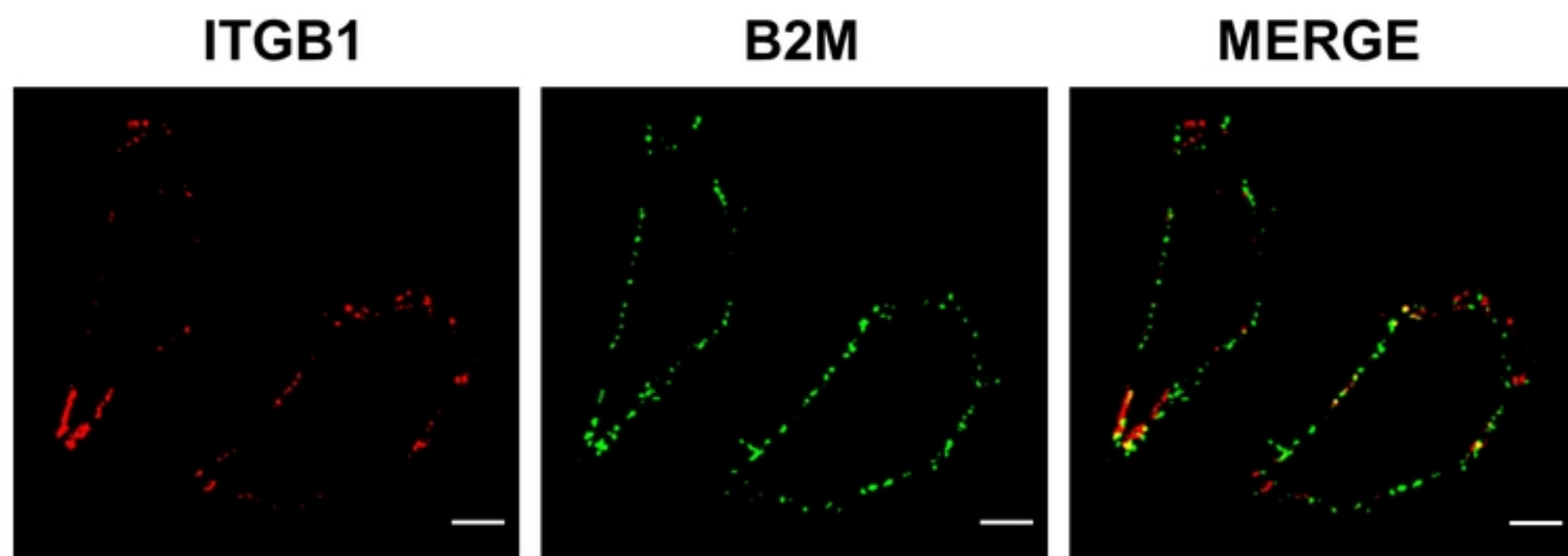
A**B**

Figure 10

